



## 2015 Mining and Mineral Symposium

May 8–10, 2015

Montana Bureau of Mines and Geology

Butte, Montana

## TABLE OF CONTENTS

Foreword.....	iii
Agenda.....	iv
Vent Deposits within the Late Cretaceous Elkhorn Mountains Volcanics of Southwestern MT <i>Kaleb C. Scarberry, Montana Bureau of Mines and Geology.....</i>	1
Porphyry Clan Deposits and Gold-Only Deposits in Cordilleran Style Orogenic Belts—Insights into the Metallogenic Differences from Ore Fluid Analysis <i>John Ridley, Department of Geosciences, Colorado State University, Fort Collins, CO.....</i>	6
Mineralogy of Selected Pegmatites, Black Hills, South Dakota <i>John L. Lufkin and Tom Loomis.....</i>	8
Minerals of Montana, A Journey Across the Treasure State <i>Michael J. Goble, P.E. Aurora, Colorado.....</i>	10
Use of Narrow Vein Mining Methods and Geologic Grade Control on the J-M Reef Palladium- Platinum Deposit <i>Sarah Jensen, Stillwater Mining Company, Nye, MT.....</i>	21
Geologic Overview and Preliminary Results: Temporal and Spatial Distribution of Auriferous Gravels Derived from the Butte District, Montana—A Consequence of Regional Tectonics and Early Paleocene Rapid Exhumation <i>Robert A. Houston, 2015.....</i>	25
Boron Minerals of Western Montana—Occurrences and Ore Deposit Models <i>Bruce E. Cox, Geologist / Consultant, Missoula, Montana.....</i>	34
Elevated REE in Ore Minerals of the Pryor Mountain Mining District, South Central MT <i>Anita Moore-Nall and David R. Lageson; Montana State University, Department of Earth Science, Bozeman, Montana.....</i>	47
Silver Mineralogy of the Butte Mines <i>Chris Gammons and Ryan Stevenson, Department of Geological Engineering, Montana Tech, Butte, MT 59701,.....</i>	50
Revised Model for Carbonate-Hosted Proterozoic Hydrothermal Talc Deposits in Southwest MT <i>S.J. Underwood, Senior Geologist, Childs Geosciences, Bozeman, Montana.....</i>	51

Boulder Batholith Pegmatites

*William C. (Chris) van Laer, ASTERISM Services, Butte, Montana..... 54*

Reserve Definition and Geology, Continental Pit, Butte Montana

*Steve Czehura, Montana Resources, LLP, Butte, MT..... 56*

Some constraints on the origin of Montana sapphire deposits

*Richard B. Berg, Montana Bureau of Mines and Geology..... 58*

## Foreword

Montana and the surrounding states have a unique geology that presents many opportunities for valuable continuing research on mineral deposits. Research centered on economic geology and mineralogy can lead to a better understanding of the mineral deposits in this region, and thus the discovery of future exploration targets that have potential for development into operating mines. Mining has long been, and will continue to be, vital to the economy of Montana and the surrounding region.

The Montana Bureau of Mines and Geology hosted its first Mining and Minerals Symposium on the Montana Tech campus, May 8–10, 2015, to provide a forum for the presentation of economic geological and mineralogical research. The symposium was designed for professionals, students, and non-professionals all to participate and present ideas. The intent of this symposium was to encourage future and ongoing economic geology research in Montana and the surrounding region, and to provide an opportunity for those conducting such research in the northwestern states to present and discuss their work.

Presentations covered a variety of topics, including ore genesis, mineralogy, mining methods, and mineral resource geology covering Montana and South Dakota. Abstracts submitted by the speakers are presented in the following meeting proceedings.

John Metesh, State Geologist  
Montana Bureau of Mines and Geology

Stan Korzeb, Economic Geologist  
Montana Bureau of Mines and Geology

## Agenda

### May 9, 2015

Elkhorn Mountains Volcanics, *Dr. Kaleb Scarberry, Associate Research Geologist, Montana Bureau of Mines and Geology*

Porphyry deposits and gold-only deposits—Insights into the differences from ore fluid compositions, *Dr. John Ridley, Associate Professor, Geosciences, Colorado State University*

Mineralogy of selected pegmatites, Black Hills, South Dakota, *Dr. John Lufkin, Consultant, Lufkin Consultants, Professor, Colorado School of Mines*

Minerals of Montana—A mineralogical journey across the Treasure State, *Michael Goble, P.E., U.S. Bureau of Reclamation*

Use of narrow vein mining methods and geologic grade control on the J-M Reef palladium deposit, *Sara Jensen, Geologist, Stillwater Mining Company*

Geology and placer gold deposits of the Butte Mining District, *Bob Houston, Economic geologist, Oregon State Survey*

Boron minerals of western Montana—Occurrences and ore deposit models, *Bruce Cox, Consulting Geologist, Mining and Mineral Exploration, Missoula, MT*

Elevated REE in ore minerals of the Pryor Mountain Mining District, south central Montana, *Anita Moore-Nall, Montana State University, Bozeman, MT*

### May 10, 2015

Mineralogy and geochemistry of Butte, Montana, *Dr. Chris Gammons, Professor, Geological Engineering, Montana Tech, Butte, MT*

Revised model for carbonate-hosted Proterozoic hydrothermal talc deposits, *Dr. Sandra Underwood, Senior Geologist, Childs Geosciences, Bozeman, MT*

Pegmatites of Montana's Boulder Batholith, *Chris van Laer, Owner, Asterism Services, Butte, MT*

Reserve definition and geology, *Steve Czehura, Manager, Engineering and Geology, Montana Resources, Butte, MT*

Montana Sapphires, *Dr. Richard Berg, Research Geologist, Emeritus, Montana Bureau of Mines and Geology, Butte, MT*

# Vent Deposits within the Late Cretaceous Elkhorn Mountains Volcanics of Southwestern Montana

*Kaleb C. Scarberry, Montana Bureau of Mines and Geology*

The east and west flanks of the Boulder Batholith expose 25,000 km<sup>2</sup> of the Elkhorn Mountains Volcanic field (Klepper and others, 1957) (Figure 1). The volcanic pile was ~4.6 km thick when it formed Smedes (1966). Ash deposits in the sequence are among the most voluminous documented on Earth (summary in Roberts and Hendrix, 2000). Up to 3 km of the section eroded away during exhumation of its plutonic root, the Boulder batholith (Klepper and others, 1957; Lipman, 1984). Vent proximal rocks are associated with Au mineralization in the Emery mining district, and at the Golden Sunlight Mine (Figure 1).

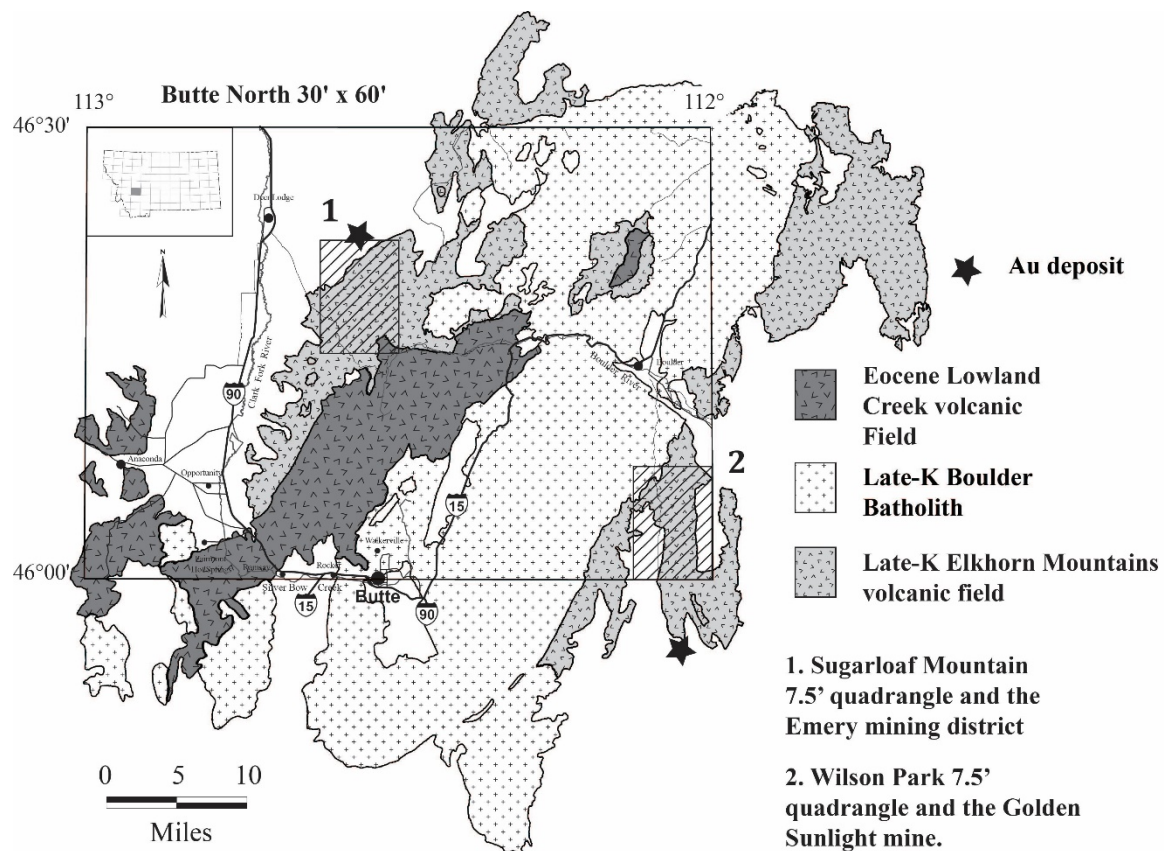


**Figure 1.** Location map shows the quadrangles and Au deposits discussed in this paper.

Field studies (Klepper and others, 1957, 1971; Ruppel, 1963; Becraft and others, 1963; Smedes, 1966; and Weeks, 1974) describe three members of the Elkhorn Mountains Volcanics.

**Lower member:** Basaltic, andesitic, and rhyodacitic pyroclastic and epiclastic volcanic rocks, such as mudflows. Also contains autobrecciated lavas, lapilli tuffs, and minor, thin, interlayered silicic ash-flow tuffs. Volcanic breccia and conglomerate increase up the section.

Clast size also increases up the section. Measured and estimated thicknesses range from 200 to 1500 m.

**Middle member:** Sheets of welded ash-flow tuff with intercalated debris from the lower member. Welded tuff alternates with ash-fall crystal tuff and subordinate thin beds of water-laid tuff. Measured and estimated thicknesses range from 450 to 2300 m.

**Upper member:** Bedded and water-laid tuff and andesitic sedimentary rocks. Includes conglomerates to mudstones with a large component of volcanic material. A few lenticular beds of fresh-water limestone and some andesite flows occur. Measured and estimated thicknesses range from 530 to 2100 m.

Dioritic rocks of varied texture and uncertain origins are common. Some of these rocks are stocks, dikes, and sills that fed the volcanic deposits. Others may be volcanic rocks recrystallized by intrusion of the batholith.

Late Cretaceous volcanic rocks are 1.5 km thick in the Sugarloaf Mountain quadrangle (Figure 1) where the lower and middle members of the Elkhorn Mountains Volcanics (Figure 2) crop out. The rocks form a subalkaline suite continuous from basaltic andesite to rhyolite ( $\text{SiO}_2$  ~52–75 wt. %). Lower member andesite ( $\text{SiO}_2$ : ~53.5–60.5 wt. %) erupted from northeast-trending fissures located in the vicinity of Sugarloaf Mountain. The fissure deposits transition outward to the north where lavas host Au-bearing quartz veins in the Emery mining district (Pardee and Schrader, 1933). The lavas are in contact with pyroclastic rhyolite ( $\text{SiO}_2$ : ~69.0–74.7 wt. %) deposits (Figure 2, middle member) south and east of the Emery mining district.

Vent wall fracturing and fluid circulation due to caldera formation could have contributed to the ore setting at the Emery mining district. The contact between andesite and rhyolite deposits in the Sugarloaf Mountain quadrangle is likely a caldera wall unconformity. The curved, north-trending contact spans the quadrangle. Densely welded ignimbrite (Figure 2, upper tuff) is buttressed against andesite fissure deposits near Sugarloaf Mountain. Collapse breccia is interstratified with the ignimbrite ~3 km to the east, at Cliff Mountain. The distribution of near vent deposits, consistent with an intra-caldera origin, suggests that the vent once occupied an area of ~95 km<sup>2</sup>.

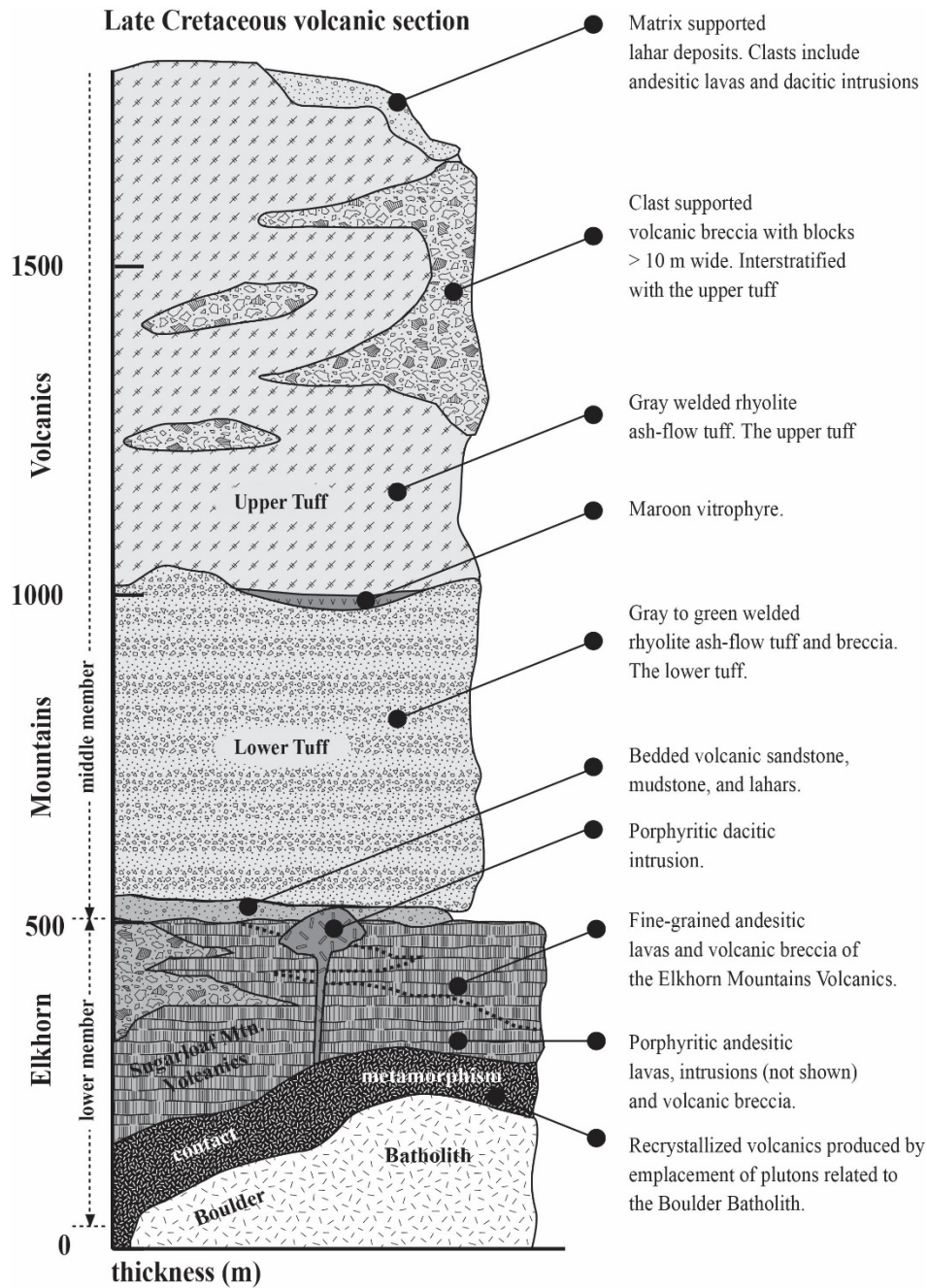


**Figure 2.** Composite section of the Elkhorn Mountains Volcanics in the Sugarloaf Mountain quadrangle.

The Golden Sunlight Mine (Figure 1) is the largest gold producer in Montana (see Oyer and others, 2014). The ore setting consists of gold-bearing rhyolite breccia that is cut by lamprophyre dikes. An emplacement age of ~80 Ma (U-Pb) is argued for the rhyolite, and lamprophyre dikes are  $76.9 \pm 0.5$  Ma ( $^{40}\text{Ar}/^{39}\text{Ar}$ ) (DeWitt and others, 1996). Both rock types are cut by the north-striking Corridor fault, a low-angle, down to east, normal fault. Yet restoring the

mineralized breccia pipe to vertical changes the Corridor fault to a low-angle, top to east, reverse fault (Oyer and others, 2014).

Geologic relationships in the Wilson Park quadrangle indicate that the ore setting of the Golden Sunlight Mine may extend northward (Figure 1). Alkalic rocks intrude and brecciate middle member rhyolite of the Elkhorn Mountains volcanic field. Layered gabbro, diorite, and syeno-diorite intrusions ( $\text{SiO}_2 = 47.9\text{--}59.7$  wt. %) (Figure 3) are overlain by near-vent lavas, breccia, and late-stage lamprophyre dikes. These coarsely porphyritic, calc-alkaline rocks form in part by assimilation of gabbro by high-temperature syenitic magma (Prostka, 1974). A structure similar to the Corridor fault occurs in the Wilson Park quadrangle. Alkalic rocks entrained in this fault contain sulfide minerals.

#	1	2	3	4	5	6	7	8	na
sample ID	KCS-14-67	KCS-14-77	KCS-14-80	KCS-14-83	KCS-14-73	KCS-14-26	KCS-14-38	KCS-14-20	CWO-14-11
map unit	Kei	Kei	Kei	Kei	Kei	Kei	Kemt	Kehi	*Kemt
XRF (wt. %)									
SiO <sub>2</sub>	51.12	55.24	55.56	47.84	59.68	51.84	60.58	51.15	61.71
TiO <sub>2</sub>	0.83	0.92	0.92	0.77	0.82	0.74	0.65	0.78	0.70
Al <sub>2</sub> O <sub>3</sub>	14.31	15.96	16.19	13.39	14.80	13.52	19.04	15.50	18.95
**FeO <sub>T</sub>	8.93	8.81	8.77	9.85	6.34	8.60	3.49	8.58	3.97
MnO	0.15	0.17	0.17	0.16	0.11	0.18	0.06	0.17	0.09
MgO	6.58	4.87	4.82	9.97	4.00	9.22	1.08	5.32	1.25
CaO	8.36	7.76	7.75	9.79	5.49	9.11	5.72	8.03	4.21
Na <sub>2</sub> O	2.46	3.07	3.17	2.25	2.86	1.69	3.08	3.15	4.54
K <sub>2</sub> O	2.98	2.11	2.11	2.96	4.35	3.37	3.42	2.94	3.08
P <sub>2</sub> O <sub>5</sub>	0.44	0.32	0.33	0.43	0.29	0.45	0.16	0.50	0.17
LOI	2.66	0.10	0.00	1.53	0.15	0.51	1.63	2.18	0.81
a.t.	96.17	99.23	99.77	97.41	98.74	98.71	97.29	96.12	98.67
Trace elements (ppm) (XRF)									
Ni	40	17	16	158	40	195	3	15	3
Cr	129	66	66	485	110	559	5	51	9
Sc	31	25	24	29	18	27	9	25	11
V	244	207	207	222	159	201	61	220	69
Ba	712	773	778	483	718	663	1258	735	1155
Rb	56	49	49	65	155	83	91	60	77
Sr	1101	1010	1042	1061	667	798	844	1471	769
Zr	86	137	137	82	252	94	269	99	290
Y	18	24	24	18	23	18	22	20	24
Nb	9	11	11	9	17	7	11	10	12
Ga	16	19	19	16	18	15	19	17	19
Cu	92	22	26	100	61	103	7	34	5
Zn	82	82	85	95	66	81	47	119	58
Pb	6	9	8	4	17	9	17	9	19
La	22	32	31	23	51	21	38	32	38
Ce	48	66	63	42	88	40	65	53	70
Th	4	7	6	4	22	4	9	6	10
Nd	25	31	28	24	36	20	28	25	29
U	1	3	3	3	5	1	2	3	2

\* Sample was collected west of the map region in the Ratio Mountain 7.5' quadrangle \*\*All Fe expressed as Fe<sup>2+</sup>  
 Analysis done at Washington State University. LOI = loss on ignition; a.t. = analytical total

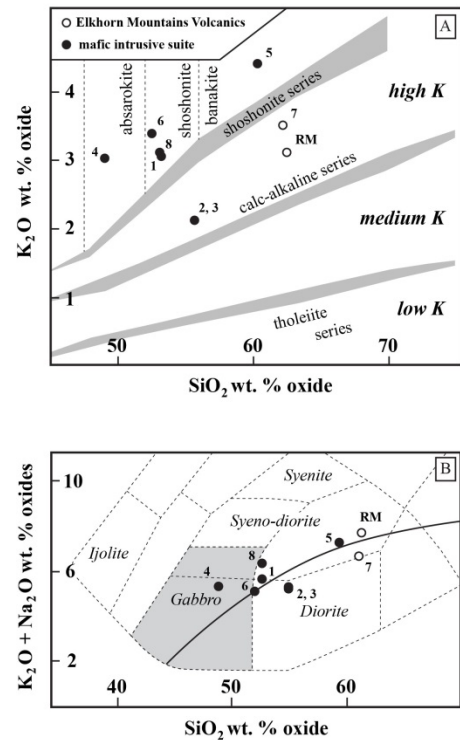


**Figure 3.** Geochemical data for high-K igneous rocks in the Wilson Park quadrangle. (A) Total alkalis versus silica (TAS) diagram after Cox and others (1979) and (B) TAS adapted for plutonic rocks by Wilson (1989). The curve on the diagram subdivides alkalic and subalkalic fields.

## References

Becraft, G.E., Pinckney, D.M., and Rosenblum, Sam, 1963, Geology and mineral deposits of the Jefferson City Quadrangle, Jefferson and Lewis and Clark Counties, Montana: U.S. Geological Survey Professional Paper 428, scale 1:48,000.

DeWitt, Ed, Foord, E.E., Zartman, R.E., Pearson, R.C., and Foster, Fess, 1996, Chronology of Late Cretaceous igneous and hydrothermal events at the Golden Sunlight gold-silver breccia pipe, southwestern Montana, U.S. Geological Survey Bulletin 2155, 48 p.

- Klepper, M.R., Ruppel, E.T., Freeman, V.L., and Weeks, R.A., 1971, Geology and mineral deposits, east flank of the Elkhorn Mountains, Broadwater County, Montana: U.S. Geological Survey Professional Paper 665, scale 1:48,000.
- Klepper, M.R., Ruppel, E.T., Freeman, V.L., and Weeks, R.A., 1971, Geology and mineral deposits, east flank of the Elkhorn Mountains, Broadwater County, Montana: U.S. Geological Survey Professional Paper 665, scale 1:48,000.
- Lipman, P.W., 1984, The roots of ash flow calderas in western North America: Windows into the tops of granitic batholiths: *Journal of Geophysical Research*, v. 89, no. B10, p. 8801–8841.
- Oyer, Nancy, Childs, John, and Mahoney, J.B., 2014, Regional setting and deposit geology of the Golden Sunlight Mine: An example of responsible resource extraction, *in* Shaw, C.A., and Tikoff, B., eds., *Exploring the Northern Rocky Mountains: Geological Society of America Field Guide 37*, p. 115–144.
- Pardee, J.T., and Schrader, F.C., 1933, Metalliferous deposits of the greater Helena mining region, Montana: U.S. Geological Survey Bulletin 842, 318 p.
- Prostka, H.J., 1973, Hybrid origin of the Absarokite-Shoshonite-Banakite series, Absaroka volcanic field, Wyoming, *Geological Society of America Bulletin*, v. 84, p. 697–702.
- Roberts, E.M., and Hendrix, M.S., 2000, Taphonomy of a petrified forest in the Two Medicine Formation (Campanian), Northwest Montana: Implications for palinspastic restoration of the Boulder Batholith and Elkhorn Mountains Volcanics: *PALAIOS*, v. 15, p. 476–482.
- Ruppel, E.T., 1963, Geology of the Basin Quadrangle, Jefferson, Lewis and Clark, and Powell Counties, Montana, U.S. Geological Survey Bulletin 1151, 121 p., scale 1:48,000.
- Smedes, H.W., 1966, Geology and igneous petrology of the Northern Elkhorn Mountains, Jefferson and Broadwater Counties, Montana: U. S. Geological Survey Professional Paper 510, 82 p., scale 1:48,000.
- Weeks, R.A., 1974, Geologic map of the Bull Mountain area, Jefferson County, Montana: U.S. Geological Survey Open-File-Report 74-354, scale 1:48,000.

# **Porphyry Clan Deposits and Gold-Only Deposits in Cordilleran Style Orogenic Belts—Insights into the Metallogenic Differences from Ore Fluid Analysis**

*John Ridley, Department of Geosciences, Colorado State University, Fort Collins, Colorado*

Cordilleran-style orogenic belts such as in western North America are hosts to multiple types of hydrothermal ore deposits—most importantly, porphyries, high and low-sulfidation epithermal, orogenic gold veins, and Carlin-type deposits. What controls where, when, and whether one rather than another deposit type forms? And what controls the variations of metal content across each deposit type? New insights into these questions are provided by results of elemental compositional data on fluid inclusions now available through laser-ablation inductively-coupled plasma mass spectrometry (LA-ICP-MS).

It is now generally recognized that porphyry, high-sulfidation epithermal and low-sulfidation epithermal deposits can all form at one longer-lived magmatic center, even if probably not simultaneously (e.g. Hedenquist et al., 1998). The differences between these deposit types are not primarily the results of differing fluid compositions at source, but are rather results of different physical mechanisms of fluid escape from upper-crustal magma chambers, the degree of interaction of the fluid with rock on ascent, and possibly phase separation in the ore fluid on ascent (e.g. Heinrich, 2005). These polymetallic deposits can thus be considered one clan. There is however a first-order division of both metallogeny and setting between these multi-element (Cu, Au, Ag, Mo) deposits and hydrothermal gold-only deposits (orogenic-gold, Carlin-type and intrusion related gold deposits – IRGD's). With respect to setting, most porphyry clan deposits form along volcanic arcs, although there are important exceptions. In contrast, although gold-only deposits are arc-related and most are associated with broadly calc-alkaline magmatism, they form in terrains of either back-arc or fore-arc magmatism.

The contrasting metal inventories of these two deposit groups were historically explained as results of, respectively, metal-poor low-salinity CO<sub>2</sub>-bearing, and metal-rich high-salinity aqueous ore fluids. However, work at Butte and elsewhere has shown that primary fluids exsolved from magma beneath porphyry deposits are relatively low-salinity, and in many cases CO<sub>2</sub>-bearing (e.g. Rusk et al., 2008), and are hence little different from the fluids of gold-only deposits, at least with respect to these parameters. Recent experiments have further shown that ore metals can be transported in such low-salinity vapour-like fluids and that high-salinity is thus not a prerequisite for metal-rich ore fluids (e.g. Hurtig and Williams-Jones, 2014).

LA-ICP-MS fluid inclusion analyses provide data on concentrations of rock-forming metals and some data on ore metals in fluids. Perhaps disappointingly the data have shown broad ranges of ore fluid composition in each deposit group, with significant overlap in the concentrations of most major metals and ore metals between the porphyry clan and gold-only deposit group (Audetat et al., 2008; Garofalo et al., 2014). This broad similarity may reflect ore fluid sourcing at similar temperatures from similar rock types, or fluids similarly equilibrated.

Fluids at all types of gold-only deposit do, however, share some unique and common characteristics, in particular, lower contents of Cu, Fe, and Mn and lower K/Na ratios compared to fluids of porphyry and related deposits. The lower Fe content is in particular significant. The similarity of the fluid at all gold-only deposit types implies uniformity of genetic processes, and hence by implication supports a magmatic origin of the ore fluid of orogenic gold deposits.

The differences between the fluid of gold-only deposits and porphyry clan deposits are difficult to conventionally explain. Iron contents, for instance, are expected to be buffered by equilibrium with iron minerals such as magnetite or ilmenite in the source rock. Although some partitioning of gold into a vapour phase relative to other metals including Cu is expected on phase separation and can explain gold-rich epithermal deposits, phase separation at high pressures would not give extreme metal fractionation so as to produce gold-only deposits. In any case phase separation would not strongly fractionate major elements such as Na, K, and Fe (Heinrich, 2007) and cannot explain the different ratios of rock-forming elements between the fluids of the two deposit groups.

One potentially important variable that may explain the differences in fluid composition, but is rarely analyzed for, and is difficult to analyze, is that of the anion, and hence ligand, content of fluids. Chloride is generally assumed to be the overwhelmingly dominant ligand, but high concentrations of carbonate and sulfur species are predicted in arc magmas at depth. Geothermal fluids with different ratios of bicarbonate to chloride are recognized, for instance at Yellowstone (Fournier, 1989). To what degree carbonate in solution can act as a ligand and contribute to the aqueous transport of metals under different conditions is unknown. The unique cation ratios of gold-only fluids are, however, qualitatively consistent with theoretical predictions of mineral solubility in fluids in which bicarbonate is an important ligand in addition to chloride. For want of a better validated explanation, it is therefore speculatively proposed that ligand inventory may differ in fluids exsolved from different magmas and that this may control metal inventory. The pathways of cycling of the different volatiles in subduction and residence in the mantle are also poorly known, but their availability may control different metal inventories of subduction-related magmas.

## References

- Audetat A, Pettke T, Heinrich CA and Bodnar RJ, 2008, *Economic Geology* 103, 877-908.
- Fournier RO, 1989, *Annual Review of Earth and Planetary Sciences* 17, 13-53.
- Garofalo PS, Fricker MB, Günther D, Bersani D and Lottici P, 2014, *Geological Society Special Publication* 402, 71-102.
- Hedenquist J, Arribas A and Reynolds J, 1998, *Economic Geology* 93, 373-404.
- Heinrich CA, 2005, *Mineralium Deposita* 39, 864-889.
- Heinrich CA, 2007, *Reviews in Mineralogy and Geochemistry* volume 65, pp 363-387.
- Hurtig NC and Williams-Jones AE, 2014, *Geochimica et Cosmochimica Acta* 136, 169-193
- Rusk BG, Reed M and Dilles J, 2008, *Economic Geology* 103, 337-334.

# Mineralogy of Selected Pegmatites, Black Hills, South Dakota

*John L. Lufkin and Tom Loomis*

The Black Hills are located in southwestern South Dakota. They are an eroded, elongate dome, about 120 mi long from Edgemont to Spearfish, 60 mi wide, and composed of a core of Precambrian quartzites, phyllites, and schists, with off-dipping Paleozoic and Mesozoic sedimentary rocks. Literally thousands of pegmatites are associated with the 1.7 Ga Harney Peak intrusion, an S-type granite. The detailed investigation of the pegmatites conducted during WWII, and published as Professional Paper 247, by Lincoln Page and 17 members of the Geological Survey, remains as a classic (Page et al., 1953).

During WWII, these pegmatites were major producers of strategic mica, lithium, and beryllium. In this presentation the mineralogy of ten pegmatites are discussed, including the Etta, Peerless, Bull Moose, Bob Ingersoll, Tin Mountain, St. Louis, Dan Patch, White Elephant, Helen Beryl, and TipTop.

The TipTop pegmatite, located 5 miles southwest of Custer, is spatially and temporally related to emplacement of the Harney Peak Granite. It is one of the most famous pegmatites in the world and currently, a total of 92 minerals have been found here (Lufkin et al., 2009). It is truly a mineralogical mecca which has been visited and studied by some of the most prominent mineralogists in the world. Its true fame lies in the present of hydrothermally (?) altered beryllium and phosphatic rocks. To date, twelve "type locality" minerals have been first described from the TipTop mine, including ehrleite, fansoleite, jahnsite, pahasapaite, parafransoleite, pararo-bertsite, robertsite, segelerite, tinsleyite, tiptopite, and whiteite. Seven of these minerals have not yet been found elsewhere in the world. Initial development of the TipTop began during the period of tin mining in the 1980s. Most of the pegmatites around the town of Custer, however, were originally located for mica. The TipTop was staked as a tin prospect sometime in the late 1880s, but throughout its history, the mine produced very little, if any, tin. It is extremely difficult to find any cassiterite ( $\text{SnO}_2$ ), the main ore of tin. Much later, about 1925, the Nevin family attempted to market the phosphate rock for its lithium content. This attempt was unsuccessful, however, since other mines with higher-grade ore were located.

The TipTop found new life as a feldspar producer, and the mining created an open-pit during the early 1940s with dimensions of 150 ft by 50 ft and a depth of 40 ft. Perthite, an intergrowth of microcline and Na-plagioclase, is the dominant mineral, especially in the intermediate zones, and quartz is second in abundance. Late stage fracture fillings and/or replacement bodies of quartz +/- albite-muscovite-microcline are evident, which were responsible for replacement textures associated with some of the later alteration. Beryl mineralization is associated with these fracture fillings and replacement bodies according to Fisher (1942). During this episode the rare beryllio-phosphates such as tiptopite and pahasapaite were possibly formed.

Today, the TipTop mine is largely idle, with the 75-ft-deep main pit flooded with 30 ft of water. The mine claim is owned by Tom Loomis ([www.dakotamatrix.com](http://www.dakotamatrix.com)), and access is granted by permission only (Lufkin et al., 2009).

Over the past 65 years, two theories have dominated the origin of pegmatites: the “vapor” model of Jahns-Burnham (1969) and the magmatic origin developed by David London. According to the Jahns-Burnham experiments with granitic melts, the magmas reach water saturation at 11.4 wt percent water, regardless of initial water content at 10 kb pressure. Once saturation is reached, ions diffuse from melt into the very low viscosity vapor (supercritical fluid), and grow into large crystals so characteristic of pegmatites.

With over forty publications based on his experimental work, London has convincingly shown that the important ingredients to large crystal growth are fluxes, primarily B, P, F, and H<sub>2</sub>O. To briefly summarize, the presence of fluxes has several effects on the pegmatite system: 1) they lower the liquidus and solidus temperature; 2) fluxes lower the viscosity of the melt, which promotes rapid growth and large crystals; 3) they increase the solubility of water in the melt, and 4) they drive the melt toward a more alkaline composition (London, 2008).

## References

- Fisher, Daniel Jerome, Preliminary report on some pegmatites of the Custer District, Report of Investigations, Department of Natural Resource Development, South Dakota Geological Survey, June 1942.
- Jahns, R.H., Burnham, C.W., Experimental studies of pegmatite genesis: I. A model for the derivation and crystallization of granitic pegmatites, *Economic Geology* 64:843-864, 1969.
- London, David; Anonymous, Abstracts with Programs – Geological Society of America, October, 2008: 336.
- Lufkin, John L. and others, Guidebook to geology of the Black Hills, South Dakota, 2009.
- Page, L.R. and others, Pegmatite investigations 1942-1945, Black Hills, South Dakota, USGS Professional Paper 247.

# Minerals of Montana, A Journey Across the Treasure State

*Michael J. Goble, P.E. Aurora, Colorado*

Known as the Treasure State, Montana is a mineral-rich region which has produced 14 minerals new to science (Table 1). The official state motto “Ora y Plata” meaning “gold and silver” and the state seal with its representation of mining tools clearly proclaim Montana’s mining origins. Montana Territory was established in 1864 as a consequence of the rapid influx of people questing for gold. In the 1860’s the area experienced many stampedes to new diggings including three “great gold rushes” to Grasshopper Creek in 1861, to Alder Gulch in 1863, and to Last Chance Gulch in 1864. These were the last of the great gold rushes in the lower 48 states and they left their mark on history.

The state is endowed with a number of mineral commodities of economic significance. Montana’s past production of arsenic, bentonite, building stone, copper, coal, garnet, sapphire and agate gemstones, gold, gypsum, limestone, lead, manganese, molybdenum, palladium, phosphate, platinum, silver, talc, vermiculite, and zinc is impressive. It also has produced small amounts of asbestos, antimony, bismuth, barite, cadmium, chrome, clays, corundum, fluorite, graphite, iron, rhodium, selenium, silicon, tellurium, tungsten, uranium, and vanadium. Mining remains an important industry in the State and its geology provides a wealth of specimens for the rock and mineral collector to enjoy. Approximately 626 different mineral species have been reported from Montana occurrences (Table 2). The occurrence of these minerals can be better understood as a function of the diverse geology of Montana. The author’s presentation will provide an overview of the state’s geology to illustrate how geology influences mineral occurrences. With this background established, we will travel from east to west again, making brief stops at significant Montana mineral localities. Although it is an oversimplification, for our east to west journey the state is divided up into the following geologic provinces:

- Great Plains Province—The eastern third of the state is dominated by sedimentary rocks and gentle terrain; the province is known for specimens of calcite, barite, gypsum, and agate and petrified wood varieties of quartz. Important mineral specimens include the extensive occurrence of Montana agate variety of quartz along and near the Yellowstone River, the orange calcite from near Alzada, the concretions containing calcite and barite crystals from the Pierre Shale in the Cedar Creek anticline, and the barite and tyuyamunite from the uranium mines in the Pryor Mountains.
- Montana Alkali Province—In the middle third of the State the sedimentary rocks have been penetrated by the intrusion of igneous rocks forming isolated mountain ranges. An uplifting action of the intrusive rocks, and other tectonic events forming the mountains, has turned the adjacent sedimentary rocks upwards, thus exposing many different sedimentary formations. The most extreme example is the Crazy Mountains, so named because the sediments are completely overturned with the older sediments lying above younger sedimentary formations. The intrusive rocks and adjacent altered sedimentary

rocks of the Montana alkali province contain both rare minerals and interesting ore deposits. Important mineral specimens include the galena, pearceite, and other sulfides from Neihart, the sylvanite from the Spotted Horse mine at Maiden, the barytolamprophyllite and other rare minerals from Gordon Butte, gem corundum (sapphires) from Yogo Gulch, and nepheline and rare silicates from the Rocky Boy stock.

- Absaroka Province—The Absaroka-Beartooth Mountains and the Gallatin Range to the west have 4 billion year old Precambrian gneiss and granite and other basement rocks (Stillwater Complex) which were uplifted during the Laramide Orogeny. Some of these rocks also experienced explosive volcanic activity dating from 53 to 48 million years ago resulting in deposits of dacite, ash-flow tuff, and rhyolite. The Absaroka Volcanics are responsible for the formation of the famous petrified forests which occur in the area. The 600,000-year-old Yellowstone caldera is a much younger eruptive center which has overprinted some of the Absaroka Volcanics. Important mineral specimens include chromite and serpentine from the Hellroaring District in the Beartooth Mountains, platinum group minerals and chromite in the Stillwater Complex, petrified wood (quartz and opal) in the Gallatin petrified forest, staurolite crystals from Crystal Cross Mountain, calcite crystals near Red Cliff campground, and hyalite variety of opal from Hyalite Ridge in the Gallatin Range.
- Wyoming Archean Province—Precambrian rocks which have been subjected to intense metamorphic action and later intruded and uplifted during the Laramide Orogeny. Important mineral specimens include almandine from the Ruby Mountains, corundum crystals from the Bear Trap, Elk Creek, Bozeman, and Sweetwater road deposits, gold and corundum from Alder Gulch, and dolomite and talc from the Yellowstone mine.
- Rocky Mountains Province—A complex geologic province which features extensive intrusion of batholiths and volcanism and uplifting associated with the Laramide Orogeny. The region includes metallic deposits and pegmatites in intrusive rocks, skarns and metallic replacement deposits formed where the intrusive rocks make contact with sediments, and metallic deposits and zeolites in volcanic rocks. Important specimens include pyrite, covellite, enargite, rhodochrosite, and other minerals from Butte, smoky and amethyst quartz, microcline, albite, and schorl in pegmatites in the Boulder Batholith, Japan law twin quartz from the PC mine, descloizite, hemimorphite, mimetite, vanadinite, and wulfenite from Radersberg, quartz, philipsburgite, veszelyite, and tetrahedrite from the Black Pine mine, rhodochrosite from Philipsburg, andradite and epidote at Pats Gulch and the Calvert mine, diopside at Bald Mountain, gold from Bannack, Last Chance, Ophir, and the Highlands districts, grossular and spinel from the Crazy Spinx claim, barite from near Basin, corundum from the Missouri River and Rock Creek, amethyst and smoky quartz from Crystal Park, and smoky quartz from Lolo Pass.
- Belt Basin Province—A sequence of metasedimentary rocks up to 50,000 feet thick. Where intruded or affected by thermal fluids interesting mineral deposits occur. Important specimens include fluorite and parasite from the Snowbird mine, boulangerite

from the Iron Mountain mine, stibnite from the Babbit mine, aramayoite, eskimoite and other sulfides from the Flathead mine, arsenopyrite crystals from the Iron Mask mine, and aegirine and vermiculite from the Zonolite mine.

Larry French published a series of publications with the title Minerals of Montana which are a bibliography of Montana mineral locality references. The author recently published a mineral locality index for the State of Montana (Gobla, 2012) in Rocks and Minerals Magazine. This work is a part of the mineral locality index of the United States, a project of the Friends of Mineralogy. A descriptive mineralogy text for the State of Montana is forthcoming.

**Table 1. Minerals First Discovered in Montana (Type Localities).**

<b>Mineral</b>	<b>Location</b>	<b>Reference</b>
Montanite	Highland Gulch	(Genth, 1868)
Colusite	Mt. View and Tramway mines, Butte	(Nelson, 1939)
Tellurobismuthite	Fairview Mine, Garnet District, and Highland Gulch	(Fronzel, 1940)
Burbankite	Big Sandy Creek	(Pecora and Kerr, 1953)
Calkansite	Big Sandy Creek	(Pecora and Kerr, 1953)
Djurleite	Leonard mine, Butte (co-type locality)	(Roseboom, 1962)
Philipsburgite	Black Pine mine	(Pecor, 1985)
Rhodium	Stillwater Complex	(Cabri and Laflamme, 1974)
Stillwaterite	Stillwater Complex	(Cabri et al., 1975)
Palladobismutharsenide	Stillwater Complex	(Cabri et al., 1976)
Keithconnite	Stillwater Complex	(Cabri et al., 1979)
Telluropalladinite	Stillwater Complex	(Cabri et al., 1979)
Joëlbruggerite	Black Pine mine	(Mills et al., 2009)
Auriacusite	Black Pine mine	(Piilonen et al., 2010)

**Table 2. Montana Minerals**

Acanthite	Actinolite	Adamite	Aegirine
Aeschynite-(Ce)	Aikinite	Åkermanite	Alabandite
Albite	Alforsite	Allanite-(Ce)	Alloclasite
Allophane	Alamandine	Altaite	Alunite
Analcime	Anatase	Ancylite (Ce)	Andalusite
Andorite	Andradite	Anglesite	Anhydrite
Anilite	Ankerite	Annabergite	Annite
Anorthite	Anthophyllite	Antigorite	Antlerite
Apjonite	Aragonite	Aramayoite	Armalcolite
Arfvedsonite	Argentojarosite	Armalcolite	Arsenbrackebuschite
Arsendescloizite	Arsenolite	Arsenopalladinite	Arsenopyrite
Arsentsumbite	Arthurite	Aspidolite	Astrophyllite
Atacamite	Atokite	Augite	Auriacusite
Aurichalcite	Autunite	Axinite-(Fe)	Azurite
Baddeleyite	Baotite	Baryte	Barytolamprophyllite
Bastnäsite-(Ce)	Bayldonite	Beaverite-(Cu)	Becquerelite
Beidellite	Belovite-(Ce)	Benitoite	Benjaminite
Benleonardite	Beraunite	Berthierite	Bertrandite
Beryl	Betekhtinite	Beudantite	“Biotite”
Birnessite	Bismuth	Bismuthinite	Bismutite
Böhmite	Boleite	Bornite	Boulangerite

Bournonite	Braggite	Braunite	Britholite-(Ce)
Brochantite	Brockite	Bromargyrite	Brookite
Brucite	Buckhornite	Burbankite	Cafetite
Calaverite	Calcioancylite-(Ce)	Calciocatapleiite	Calcite
Caledonite	Calkinsite-(Ce)	Cancrinite	Carbocernaite
Carlsbergite	Carminite	Carnotite	Carrollite
Cassiterite	Catapleiite	Cebollite	Celadonite
Celestine	Cerussite	Cervanite	Cervelleite
Chabazite-Ca	Chalcanthite	Chalcocite	Chalcophanite
Chalcopyrite	Chalcosiderite	Chamosite	Chenevixite
Chesterite	Chevkinite-(Ce)	Chlorapatite	Chlorargyrite
Chloritoid	Chondrodite	Chromite	Chrysocolla
Chrysotile	Cinnabar	Clausthalite	Clinochlore
Clinoclase	Clinoenstatite	Clinohumite	Clinojimthompsonite
Clinosafflorite	Clinozoisite	Clintonite	Cobaltite
Coffinite	Coloradoite	Columbite-(Fe)	Colusite
Conichalcite	Connellite	Cookeite	Copperite
Copiapite	Copper	Coquimbite	Cordierite
Corkite	Cornwallite	Coronadite	Corrensite
Corundum	Cosalite	Covellite	Creaseyite
Crichtonite	Cristobalite	Cryptomelane	Cubanite
Cumingtonite	Cuprite	Cuprotungstite	Dalyite
Danburite	Datolite	Davanite	Davidite-(Ce)

Descloizite	Devilline	Diamond	Diaspore
Dickite	Digenite	Diopside	Djerfisherite
Djurleite	Dolomite	Dravite	Duftite
Dugganite	Dumortierite	Dyscrasite	Ecdemite
Edenite	Elbaite	Elpidite	Emplecite
Empressite	Enargite	Enstatite	Epidote
Epsomite	Erionite-(Ca)	Erythrite	Eskimoite
Euchroite	Eudialyte	Euxenite-(Y)	Famatinite
Faujasite	Fayalite	Ferberite	Feroxyhyte
Ferrimolybdite	Ferro-actinolite	Ferro-anthophyllite	Ferro-edenite
Ferroxahydrate	Ferro-hornblende	Ferropargasite	Ferrosilite
Fersmite	Fluocerite-(Ce)	Fluorapatite	Fluorapophyllite-(K)
Fluorcaphite	Fluorite	Fluororichterite	Fornacite
Forsterite	Francevillite	Franklinite	Freibergite
Friedrichite	Gahnite	Galena	Galenobismutite
Gartrellite	Gedrite	Gehlenite	Geocronite
Gersdorffite	Gibbsite	Giuseppettite	Gladite
Glauconite	Glaucofanite	Goethite	Gold
Goldfieldite	Goslarite	Götzenite	Graphite
Greenockite	Grossular	Grunerite	Gustavite
Gypsum	Halite	Halloysite	Halotrichite
Hammarite	Hastingsite	Häuyne	Heazlewoodite
Hedenbergite	Hedleyite	Helvine	Hematite

Hemimorphite	Henrymeyerite	Hercynite	Hessite
Hetaerolite	Heulandite	Hidalgoite	Hinsdalite
Hisingerite	Hollandite	Hollingworthite	Huanghoite-(Ce)
Hübnerite	Humite	Hydrobiotite	Hydrohetaerolite
Hydroxylapatite	Hydrozincite	Hypersthene	Ice
Idaite	Illite	Ilmenite	Ilsemannite
Imitérite	Iron	Isoferroplatinum	Jalpaite
Jarosite	Joëlbruggerite	Jordanite	Joséite-B
Kaersutite	Kalborsite	Kalinite	Kalsilite
Kaolinite	Kassite	Keithconnite	Kentbrooksite
Kermesite	Kiddcreekite	Kipushite	Kobellite
Kotulskite	Krennerite	Krupkaite	Kuksite
Kyanite	Lamprophyllite	Langite	Lanthanite-(Ce)
Laumontite	Laurite	Lazulite	Leadhillite
Lenaite	Lepidrococite	Lepidolite	Leucite
Leucoxene	Libethenite	Liebegite	Lillianite
Linarite	Lindgrenite	Lindströmite	Litharge
Lizardite	Löllingite	Loparite-(Ce)	Ludwigite
Luzonite	Mackinawite	Maghemite	Magnesio-arfvedsonite
Magnesiochromite	Magnesio-hastingsite	Magnesio-hornblende	Magnesio-riebeckite
Magnesite	Magnetite	Malachite	Mallardite
Manganite	Manganoneptunite	Marcasite	Margarite

Marialite	Marshite	Massicot	Matildite
Maucherite	Mawbyite	Mawsonite	Mckinstryite
Meionite	Melanterite	Melliniite	Melonite
Meneghinite	Menshikovite	Mercury	Merenskyite
Mertieite II	Merwinite	Mesolite	Meta-autunite
Metatorbernite	Metatyuyamunite	Metauranocircite-I	Metazeunerite
Miargyrite	Michenerite	Microcline	Millerite
Mimetite	Minium	Minnesotaite	Mirabilite
Molybdenite	Molybдите	Monazite-(Ce)	Moncheite
Montanite	Monticellite	Montmorillonite	Mooihoekite
Mordenite	Mottramite	Mukhinite	Mullite
Murdockite	Muscovite	Nabalamprophyllite	Nacrite
Nagyágite	Narsarsukite	Natrojarosite	Natrolite
Natron	Nepheline	Neptunite	Nickle
Nickeline	Nitre	Nontronite	Nordstrandite
Nosean	Nsutite	Okenite	Olivenite
Olsacherite	Opal	Orpiment	Orthoclase
Ottrelite	Oxyplumboroméite	Palarstanide	Palladium
Palladoarsenide	Palladobismutharsenide	Palygorskite	Paolovite
Paragonite	Pargasite	Parisite-(Ce)	Pearceite
Pectolite	Pentahydrate	Pentlandite	Periclase
Perovskite	Petrovskaité	Petzite	Pharmacosiderite
Phenakite	Philipsbornite	Philipsburgite	Phillipsite-Ca

Phlogopite	Phosphuranylite	Pickeringite	Piemontite
Pigeonite	Pilsenite	Pitiglianoite	Platinum
Plattnerite	Plumbojarosite	Plumbopalladinite	Polybasite
Potarite	Powellite	Prehnite	Priderite
Proustite	Pseudoboléite	Pseudobrookite	Pseudomalachite
Pumpellyite (Mg)	Pyargyrite	Pyrite	Pyrochlore
Pyrolusite	Pyromorphite	Pyrope	Pyrophanite
Pyrophyllite	Pyrosmalite-(Fe)	Pyrostilpnite	Pyrrhotite
Quartz	Ramsdellite	Raspite	Realgar
Rectorite	Rhodium	Rhodochrosite	Rhodonite
Richterite	Riebeckite	Rinkite	Romanèchite
Römerite	Rosasite	Roscoelite	Rustenburgite
Rutherfordine	Rutile	Samarskite-(Y)	Sanidine
Saponite	Scawtite	Scheelite	Schorl
Schorlomite	Schwertmannite	Scolecite	Scorodite
Segnitite	Seligmannite	Semseyite	Sénarmontite
Sepiolite	Shcherbakovite	Siderite	Siderotil
Siegenite	Sillimanite	Silver	Smithsonite
Sodalite	Sperrylite	Spessartine	Sphalerite
Spinel	Spodumene	Stannite	Stannoidite
Staurolite	Stellerite	Stephanite	Stetefeldtite
Stibiconite	Stibiopalladinite	Stibnite	Stilbite-Ca
Stillwaterite	Stilpnomelane	Stolzite	Strashimirite

Stromeyerite	Strontianite	Strontiochevkinite	Stützite
Sulfotsumoite	Sulphur	Sylvanite	Synchysite-(Ce)
Synchysite-(Y)	Szomolnokite	Talc	Talnakhite
Tantalite-(Fe)	Tarkianite	Telargpalite	Tellurium
Tellurobismuthite	Telluropalladinite	Temagamite	Tennantite
Tenorite	Tetradymite	Tetraferroplatinum	Tetrahedrite
Thenardite	Thomsonite-Ca	Thorianite	Thorite
Thortveitite	Titanite	Tobermorite	Todorokite
Topaz	Torbernite	Tremolite	Tridymite
Troilite	Tschermakite	Tsumebite	Tsumoite
Tulameenite	Tungstite	Turquoise	Tyuyamunite
Uraninite	Uranocircite-II	Uranophane- $\alpha$	Uranophane- $\beta$
Uvarovite	Uytenbogaardtite	Valentinite	Vanadinite
Vauquelinite	Vermiculite	Vesuvianite	Veszelyite
Violarite	Vivianite	Voglite	Volkonskoite
Voltaite	Vysotskite	Wadeite	Wavellite
Whewellite	Willemite	Willemseite	Winchite
Witherite	Wittichenite	Wollastonite	Woodhouseite
Wroewolfeite	Wulfenite	Wurtzite	Wustite
Xanthoconite	Xenotime-(Y)	Xonotlite	Zeunerite
Zincite	Zincrosasite	Zircon	Zoisite
Zunyite	Zvyagintsevite		

## References

- French, L.B. (2005b) Minerals of Montana Part I, Granite County, Mineral County, Missoula County, Powell County, Ravalli County. Montana Bureau of Mines and Geology Open-File Report 519, 150 p.
- French, L.B. (2007a) Minerals of Montana Part II, Beaverhead, Flathead, Lake, Lincoln, and Sanders Counties. Montana Bureau of Mines and Geology Open-File Report 519, 161 p.
- French, L.B. (2007b) Minerals of Montana Part III, Deer Lodge, Jefferson, Madison, and Silver Bow Counties. Montana Bureau of Mines and Geology Open-File Report 519, 219 p.
- French, L.B. (2008) Minerals of Montana Part IV, Broadwater, Cascade, Gallatin, Lewis and Clark, Meagher, and Park Counties. Montana Bureau of Mines and Geology Open-File Report 519, 176 p.
- French, L.B. (2009) Minerals of Montana Part V, Eastern Montana. Montana Bureau of Mines and Geology Open-File Report 519, 216 p.
- Gobla, M.J. (2012) Montana mineral locality index. *Rocks and Minerals*, 87: 208–240.

## **Use of Narrow Vein Mining Methods and Geologic Grade Control on the J-M Reef Palladium-Platinum Deposit**

*Sarah Jensen, Stillwater Mining Company, Nye, MT*

Stillwater Mining Company (SMC) is the only U.S. producer of platinum group metals (PGMs) and the largest primary producer outside of South Africa and the Russian Federation. SMC conducts underground mining operations at the Stillwater and East Boulder mines located in south-central Montana along the J-M reef, a narrow Pt/Pd sulfide horizon in the Stillwater Complex. Narrow vein mining methods and geologic grade-control procedures are utilized at SMC's mines to achieve economic retrieval of PGMs.

### **Geology of the Stillwater Complex**

The Stillwater Complex is a 2.7 billion year old differentiated stratiform mafic to ultramafic intrusive igneous body located on the northern edge of the Beartooth Range, south-central Montana. The exposed portion has a strike length of about 30 mi with a maximum width of 5 mi. It intruded 6 to 9 mi beneath the surface, resulting in a sub-horizontal inward-dipping cumulate layered lopolith. During Laramide uplift of the Beartooth block, the edge of the complex was brought to the surface and rotated by thrust faulting. Consequently these well-pronounced layers are dipping steeply to the north, although the dip angle varies throughout the complex and in some areas is overturned.

The stratigraphic classification of the Stillwater Complex is divided into three series: Basal, Ultramafic, and Banded. The Basal Series is comprised of contact-related dikes and sills and bronzitite totaling 160 to 800 ft. The Ultramafic Series consists of harzburgite and upper bronzitites totaling 4000 to 6000 ft. The Banded Series is a 16,000 ft succession of plagioclase-rich cumulates divided into six megacyclic units. The complex contains sulfide horizons associated with the Basal series and the lowermost Ultramafic Series, which have been extensively explored as a source of copper and nickel since the late nineteenth century. Chromite-rich Ultramafic Series peridotites have also been extensively explored and were effectively, but not economically, mined intermittently from 1939 to 1961. In 1973 the narrow olivine and sulfide-bearing J-M reef package was discovered by Johns-Manville Corporation geologists. Located in Troctolite-Anorthosite Zone 1 (TAZ 1) of the Banded Series, the J-M reef contains disseminated base-metal pathfinder sulfides: chalcopyrite, pentlandite and pyrrhotite, which are associated with microscopic platinum (Pt), palladium (Pd), and nickel sulfides. The most abundant minerals present are braggite, cooperite, and vysotskite with minor moncheite and Pt-Fe alloy. Metals within the J-M reef are primarily Pd and Pt at a 3.4:1 ratio. Also recovered are by-products of rhodium, copper, nickel, gold and silver.

The J-M reef is broadly continuous across the entire complex, but remarkably variable in detail. PGM-bearing minerals are restricted stratigraphically to narrow zones, but with pinches and swells, averaging 4 ft wide. Due to fault repetition there are stacked mineral zones in some areas along the reef; elsewhere, it is thinned by the same system of high-angle reverse faults, which are nearly coplanar with the igneous layering. Ballrooms, or unusually wide mineralized areas, have been discovered and mined up to 120 ft wide. The distribution of sulfide mineralization within the reef package is erratic, inconsistent, and often unpredictable. There are also differences in morphology and composition of PGMs within different host rocks. Geologists have been challenged to explain this thin, irregular, quasi-stratabound, PGM-rich horizon of the Stillwater Complex, but even more challenging is to efficiently and economically mine it.

### **Narrow Vein Mining Methods**

The primary access drift, or footwall lateral (FWL), runs parallel to the ore zone of the reef, typically 130 ft south. Mining levels at the Stillwater mine are spaced 300 ft vertically apart. Development diamond drilling is performed at 50 ft centers along the FWLs to obtain information about the reef. Geological characteristics, particularly ore grade and thickness, as well as pertinent engineering data such as rock strength and ground conditions obtained from diamond drilling, are used in determining stope design. At the Stillwater mine, only about 40% of the strike length of the J-M Reef meets economic criteria and is turned into a stoping block. SMC utilizes a variety of selective narrow vein mining methods at both of its Stillwater and East Boulder mines, including: ramp and fill, captive cut and fill, sub-level, and backstopping.

### **Ramp and Fill: Overhand & Underhand**

Ramp and Fill stopes are currently the most common production method at both of SMC's mines and account for approximately 80% of tonnage. This design is used for an intermediate to high-grade ore body, produces intermediate to high tonnage, requires a moderate amount of secondary development, and is relatively mechanized. Both jackleg and single-boom jumbos are used for drilling. Load-haul-dump (LHD) machines, or muckers, are used for moving the blasted rock (muck) from the face to a designated (ore or waste) muckbay or borehole chute. The muckers usually have 1.5 to 2 yd buckets in ramp and fill stopes, although in unique situations the ore width can justify using up to a 4 yd bucket. Typically, muckers need 6.5 to 8 ft minimum widths. Oftentimes it is the drilling configuration of the single-boom jumbo that determines the minimum mining width. Advances are generally made in 9 ft intervals, except in poor ground conditions where short rounds of 6 or 4 ft are required. Once a cut has been mined out in an overhand ramp and fill stope, it is then backfilled with waste rock or sand to become the floor for the next horizontal cut, moving upward in 10 ft intervals. Underhand ramp and fill stopes are commonly used in very poor ground conditions. Once a floor has been mined out, the cut is filled with paste, which is comprised of mill tailings and cement. Mining of the next floor commences downward in 10 ft intervals—under the previous floor.

### **Captive Stope Mining: Borehole & Alimak**

When the ore body is narrow and vertical, but has a limited extent horizontally, captive stope mining is the most economic. The ore needs to be high-grade with minimal waste, as waste and ore rounds are not separated. Captive, or slusher stopes, are accessed with an Alimak climber or a ladder in a borehole. Jacklegs are used for drilling the face, advancing in 6 ft intervals. Buckets connected to a slusher move the muck to an ore chute. Once a floor is mined out in a borehole slusher stope, a raise up to the next floor is mined and the cut is sanded, moving upward in 10 ft intervals. In an Alimak captive stope, walls are built to contain the sand, the cut is sanded, and mining commences upward in 10 ft intervals. Captive stopes are advantageous since a slusher bucket is used instead of a mucker, reducing the minimum width to 5 ft. Not only does this decrease the amount of dilution in narrow ore zones, but it drastically reduces mining costs because less equipment is needed, and it requires almost no secondary development.

### **Sub-level Mining and Backstopes**

In areas where the ore zone is reasonably straight and has proven ore-grade continuity throughout, a 30 to 40 ft panel is mined between sills along the dip of the ore body using a long-hole drill. Ore zones as narrow as 3 ft wide have been successfully mined this way. Remote muckers are used to retrieve the muck. Open panels are gobbed with waste upon completion. It is a quick, effective, and highly cost-effective narrow vein mining method. Similarly, backstopes are mined like panels within ramp and fill and occasionally captive stopes. Where the ore body is proven and consistent, it is more economical to mine a 30 ft backstope instead of three ramp and fill cuts.

### **Grade-Control Procedures**

In addition to development, production, and special projects geologists, SMC employs “grade-control” geologists who work underground at both of SMC’s mines. They have a unique responsibility to identify the ore and help guide miners to efficiently extract the mineralized rock with minimal dilution and deletion along an often difficult-to-identify hanging wall contact. The goal is to maximize ounce production at the highest possible grade within the ground rules of the chosen mining method. Because of the irregularities and unpredictability of the J-M reef and PGM mineralization, grade-control geologists are called to “mark up” every active mining face in order to achieve maximum profitability. Typically the Stillwater mine has 80 to 100 active faces and grade-control geologists will mark up 40 to 50 per day.

Once a round is bolted the miner will call a geologist to mark up the face. Ensuring that the face is safe by taking measures to bar down any loose rocks, check bolting standards, and watch for other hazards, he/she maps the face—notating location, dimensions and azimuth of the round, lithologies in the face and ribs, dip of the layered units and/or hanging wall contact, and any structural offsets or major faults. Identifying the hanging wall contact, which is the upward boundary of mineralization, and understanding the different lithologies are necessary to ensure

that mining proceeds only on the reef. The geologist then identifies the ore, determines the ore width, samples the face, and estimates the face grade based on visual sulfides, as there is a strong correlation between the volume percent visual base-metal sulfides and PGM grade content. He/she marks up the face and/or rib slabs using paint to show the miners specifically where, how wide, and in what direction to mine the next round, and whether to send the muck as ore or waste. Often, grade-control geologists discover additional ore zones between the diamond drillhole centers, which could have been missed otherwise. This produces extra ounces not accounted for in the proven reserve.

Through waste gaps to massive high-grade ballrooms, SMC geologists have been effectively and economically guiding the mining along the J-M reef since continuous production commenced in October 1985 by keeping the drifts narrow and to profile, and by making educated decisions one face at a time. The use of narrow vein mining methods and the experience and education of the geologists who navigate the mining are equally paired with the talent, skill, and hard work of the miners breaking rock every day, resulting in the profitable extraction of PGMs from the J-M reef in the Stillwater Complex.

# **Geologic Overview and Preliminary Results: Temporal and Spatial Distribution of Auriferous Gravels Derived from the Butte District, Montana—A Consequence of Regional Tectonics and Early Paleocene Rapid Exhumation**

*Robert A. Houston, 2015*

Early in the summer of 1864, auriferous gravels discovered in a gulch draining a small desolate hill in southwest Montana drew scores of hopeful prospectors to a new mining camp at Butte. Placer mining soon intensified within the gulches draining the hill and along Silver Bow Creek downstream to Rocker (Fig. 1; McLaughlin, 1934). However, within three years the town nearly became deserted after merely ~120,000 troy ounces (toz) of detrital gold was recovered (Weed, 1912). Undeterred, the remaining few soon recognized and proceeded to develop nearby outcrops of rich ore veins. The Butte District soon became known for its extensive network of massive polymetallic base metal lode veins. Later, significant porphyry Cu-Mo and supergene deposits were recognized. Additionally, the district served an important role in the formulation of new hypotheses on geologic processes that produce magmatic-hydrothermal copper deposits. However, likely as a result of very low production and grades, gold has failed to receive a robust investigation. The following presents a synthesis of Butte's geologic data merged with regional paleosedimentation records to elicit and quantify the temporal mass distribution of gold eroded from the source rocks during four important periods: early Paleocene to early Eocene, early Eocene to middle Miocene, middle Miocene to late Neogene, and late Neogene to present.

The protore deposits are hosted by the 76.3 Ma Butte Granite, the largest pluton of the late Cretaceous (82 to 74 Ma) Boulder batholith. Present day surface exposures of the granite crystallized at a depth of 5.6 to 9.5 km. Porphyry Cu-Mo and lode deposits, associated with emplacement of quartz porphyry dikes, formed in a period from 66 to 62 Ma, synchronous with Laramide compressional deformation (Fig. 1).

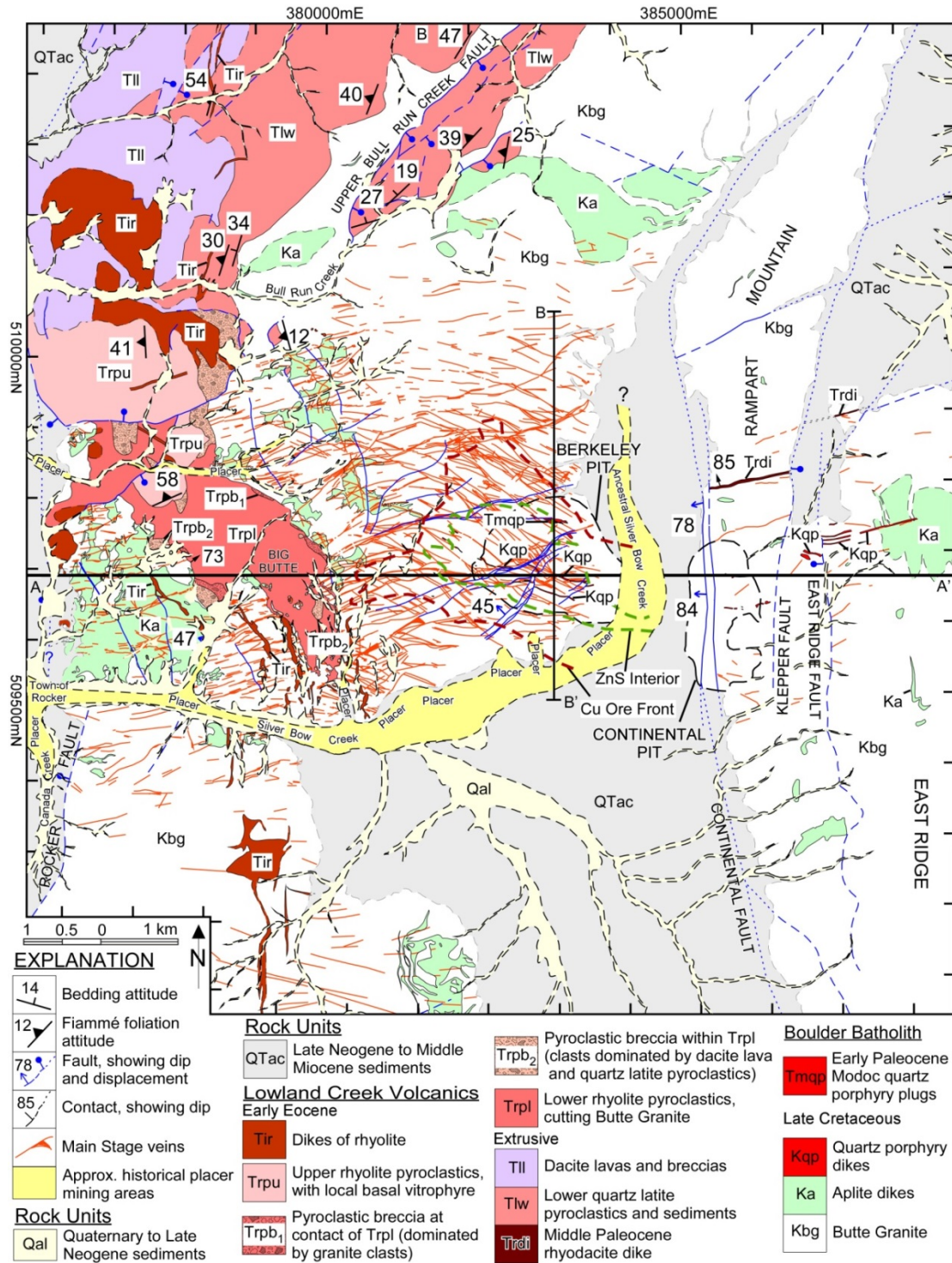


**Figure 1.** Generalized geologic map of the Butte district, Montana, showing major rock units, faults, Main stage lode veins, and approximate historical placer mining locations. Cross sections are shown in Figures 2 and 3.

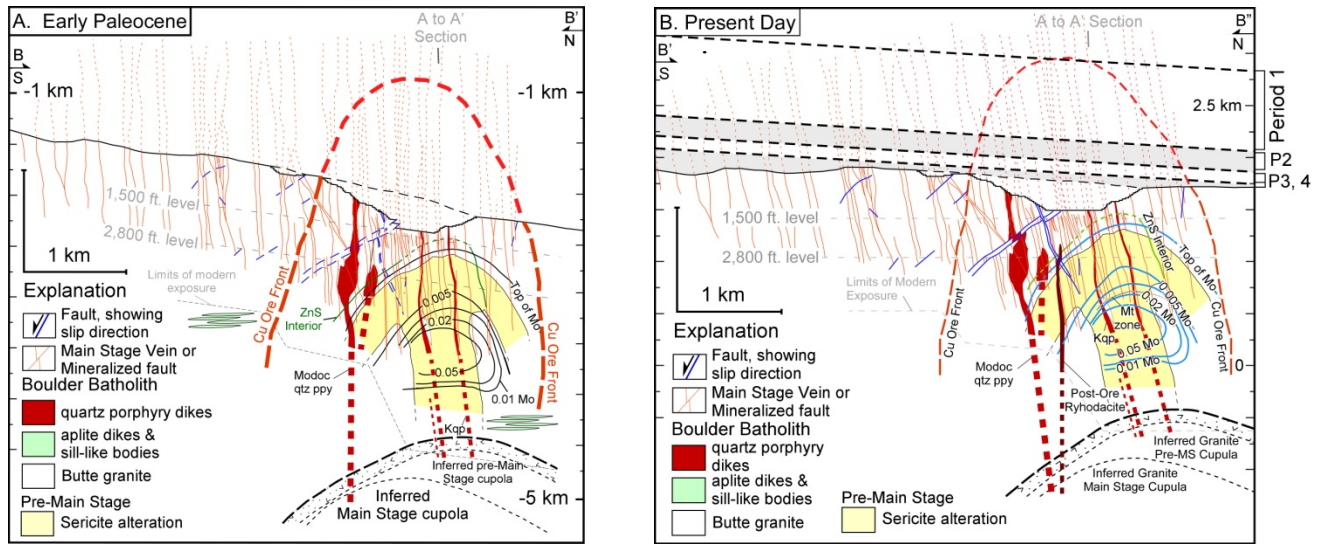


Figure 2. North-south cross section of the Butte District, showing: A. restored early Paleocene vertical emplacement orientation and vertical projection of the lode vein ore body. Early pre-Main stage porphyry Cu-Mo ores formed two domes (~66 and 64 Ma) at relatively great depths (~5–9 km) and at temperatures of 575° and 650°C (Fig. 3; Rusk et al., 2008). B. present-day cross section and four periods of protore source rock erosion. Cross section location (B to B') shown in Figure 1. Abbreviations: Ba = Badger Shaft; Cu = copper; Kqp = quartz porphyry dike; Mo = molybdenite; ppy = porphyry; qtz = quartz; ZnS = Zinc.

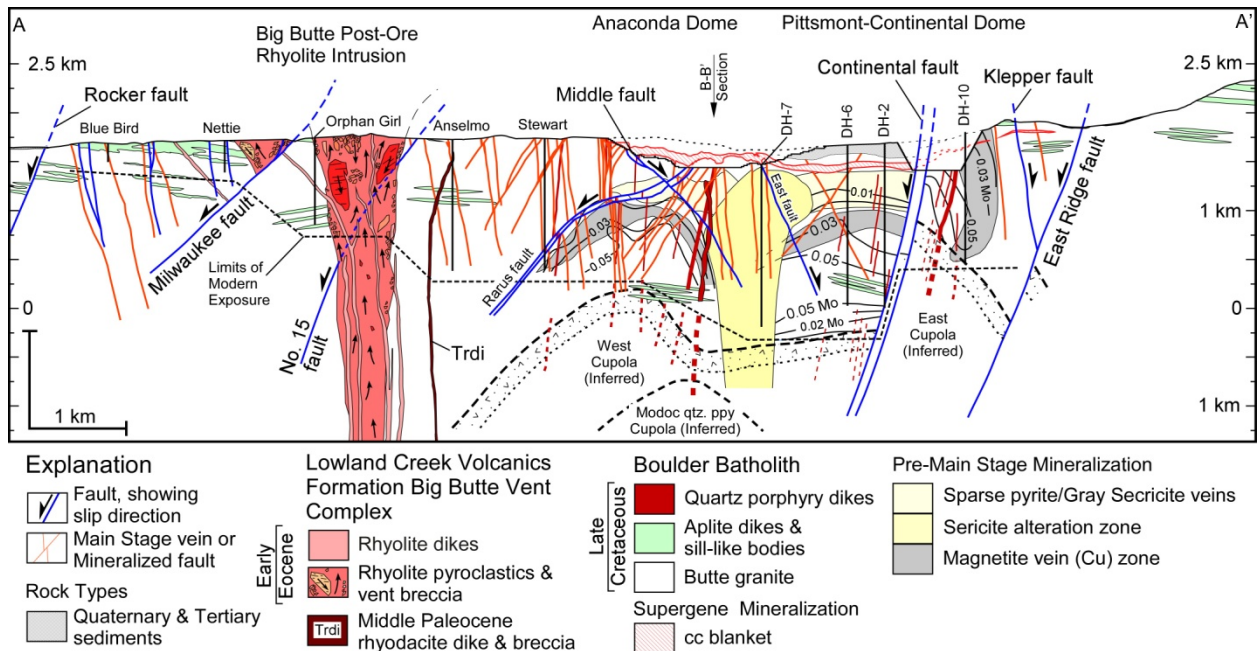


Figure 3. Present day east-west geologic cross section of the Butte District. Cross section location (A to A') shown in Figure 1. Mineral abbreviations: Mo = molybdenite.

A large central “gray sericite” zone (~64 Ma) of pervasively quartz-sericite-pyrite-altered rock occurs between and partially overprints the tops of the two pre-Main stage domes (Fig. 2). Ore fluids with similar composition evolved into slightly younger (~63.5–62 Ma) Main stage lode ores (Reed et al., 2013). The lode ores occupy two conjugate oblique-slip normal fault systems and are inferred to have formed at shallower depths (~2–6 km) and cooler temperatures (230° and 400°C) with no evidence of boiling (Rusk et al., 2008). These faults with minor displacements likely resulted from brittle failure caused by doming above a volatile-rich and buoyant granitic magma at depth. Exhumation began between 66 and 64 Ma and was very rapid during formation of gray sericite and Main stage mineralization (Houston and Dilles, 2013a). Exhumation was largely completed by the time of emplacement of the ~59 Ma rhyodacite dike. Regional deformation, during and after ore formation, gently tilted the deposit 20° ( $\pm 10^\circ$ ) northeastward. The telescoping of pre-Main stage ores by Main stage veins is driven by Laramide shortening and uplift but likely was equally influenced by the presence of easily erodible hydrothermally altered rocks above the deposit. Within ~10 m.y. following mineralization the lode veins were exposed at surface then likely buried to a depth up to 1800 m by the early Eocene Lowland Creek Volcanics Formation. Volcanism is synchronous with the transition to regional extensional faulting. Northwest from Butte, normal faulting moderately (10° to 50° NW) tilted the volcanics (Fig. 1; Houston and Dilles, 2013b). Reduced unroofing exhumed the lode veins prior to the initiation of middle Miocene Basin and Range-type normal faulting, which continues to this day. Approximately 15° east–southeast tilting by reverse drag associated with 1.3 km of normal displacement along the Continental fault marks the final tilting episode in the district. Chemical and physical weathering of the protore source mobilized the soluble ores into a supergene enrichment blanket and transported the insoluble ores into thin placer deposits surrounding the Butte Hill.

Between 1880 and 2010, production totaled ~11.3 million metric tonnes (Mt) Cu, 2.9 Mt Zn, 1.7 Mt Mn, 0.4 Mt Pb, ~0.16 Mt Mo, 22,000 t Ag, and 82.85 t Au (Long, 1995; Czehura, 2006). Reserves are estimated at 4.9 billion metric tonnes (Bt) of ore containing 0.49% Cu, and 0.033% Mo (Czehura, 2006). With respect to gold, grades range from 100 to 443 ppb in Main stage lode ore sampled from the Nettie mine dump and Cambers mines (Weed, 1912; Dilles, unpub. data). Similar grades occur between the Leonard to the Colusa and the Leonard to the Pennsylvania. Locally, grades as high as 0.36 oz/t (10 ppm) are reported for certain ore shoots in the Silver King mine (Weed, 1912). Free gold is rare, but occurs in some silver ores and is observed on chalcocite crystals from the Leonard mine. Gold occurs at very low concentrations (nil up to 15 ppb; Dilles, unpub. data) in the pre-Main stage ores, at grades similar to fresh non-mineralized Butte granite (0.6 ppb Au; Gottfried et al., 1972), and is not a likely significant source contributor. Based on ore grades, production, and reserve estimates, the ~2.6 Bt lode vein ore body contained ca. 754 tonnes of gold at an average grade of 290 ppb.

To quantify the amount of gold eroded from the deposit, the deposit is structurally restored and the lode vein ore body is vertically projected to conservatively estimate the extent of mineralization at the time of early Paleocene emplacement (Fig. 2A). Open space vein textures

and fluid inclusion pressure estimates suggest that the 2 to 6 km lode vein emplacement depth was above the ductile-brittle transition and transitional to the epithermal environment. Additionally, the restored vertical emplacement orientation of Main stage veins, prior to NE tilting, reveals that the depth of erosion is ~700 m greater in the central part than in the northern peripheral part of the district (Fig. 2A). These observations, compared to reconstructions of less-eroded porphyry copper deposits (e.g., Ann-Mason, Nevada; Dilles et al., 2000; Bajo de la Alumbrera, Argentina; Proffett, 2003; Bingham, Utah; Gruen et al., 2010; El Salvador; Gustafson and Hunt, 1975) and accepted emplacement models (Sillitoe, 2010), suggest the lode vein ore body and associated gold grades could be conservatively projected ~1 km vertically (Fig. 2A). Therefore, the late Paleocene lode vein ore body contained a total of ~1,315 t of gold (42.2 Mtoz); of which ~561 t of gold (18 Mtoz) was eroded from the source during four important periods (Fig. 2B).

**Period 1 - Early Paleocene to Early Eocene:** The paleodrainage during the early Paleocene to early Eocene directed distinctive lithologies of the northern Golden Spike Formation and the southern Beaverhead Group along a south- to southeast flowing paleovalley that joined the Beaverhead-Harebell-Pinon mega fan in the Wyoming foreland basin (Fig. 4B; Schwartz and Schwartz, 2013). During this period, 7 km of rock, comprised of (3.2 to 4.6 km) Elkhorn Mountains Volcanics and Butte granite, was ( $0.5$  to  $2 \text{ mm yr}^{-1}$ ) eroded to exposed lode veins at surface. Of this amount, ~0.75 km (vertical) of the lode ore body containing ~421 t of gold was eroded from the deposit (Fig. 2B, 4A) and conveyed southward in the paleofluvial drainage system.

**Period 2 - Eocene to Middle Miocene:** The early Eocene represents a time of transition to extensional faulting, renewed volcanism, and decreased exhumation rates. Locally, the eruption of the Lowland Creek Volcanics likely buried the district up to 1,800 m. Exposures of granitic gravels, bedded directly on deeply weathered Butte granite in the hanging wall of the Continental fault, indicate that the volcanic cover was completely removed to expose and erode the lode vein ore body prior to the commencement of middle Miocene Basin and Range-type normal faulting. The paleodrainage system in western Montana likely changed during the Eocene as the divide likely shifted southeastward from Bearmouth to an area near Anaconda (Fig. 4B). South of the divide, regionally including the Butte area, distinctive lithologies of the Renova Formation were transported southward to merge with the ancestral Missouri River system (Fig. 4B; Schwartz and Schwartz, 2013). On removal of the volcanic cover, 84 tons of gold contained in ~0.15 km of lode vein ore body was eroded from the district and entered the southward directed paleofluvial system (Fig. 2B, 4B).

**Period 3 - Middle Miocene to Late Neogene:** The final stages of placer development at Butte is marked by the commencement of middle Miocene Basin and Range-type extensional faulting that altered the paleodrainage system across SW Montana. Locally, the district resides in the northern part of an east to southeastward tilted half horst and graben structure. During this time, the ancestral Silver Bow Creek directed auriferous gravels westward into the Rocker basin, then southward into the Beaverhead graben to merge with the ancestral Missouri River system

(Fig. 4C; Sears and Ryan, 2003; Vuke, 2004; Sears et al., 2009; Schwartz and Schwartz, 2013). As a result of basin development and reduced unroofing in the hanging wall of the Continental fault, approximately 0.075 km of the lode vein ore body containing 42 t of gold was eroded and conveyed into the middle Miocene paleofluvial drainage system (Fig. 2B, 4C).

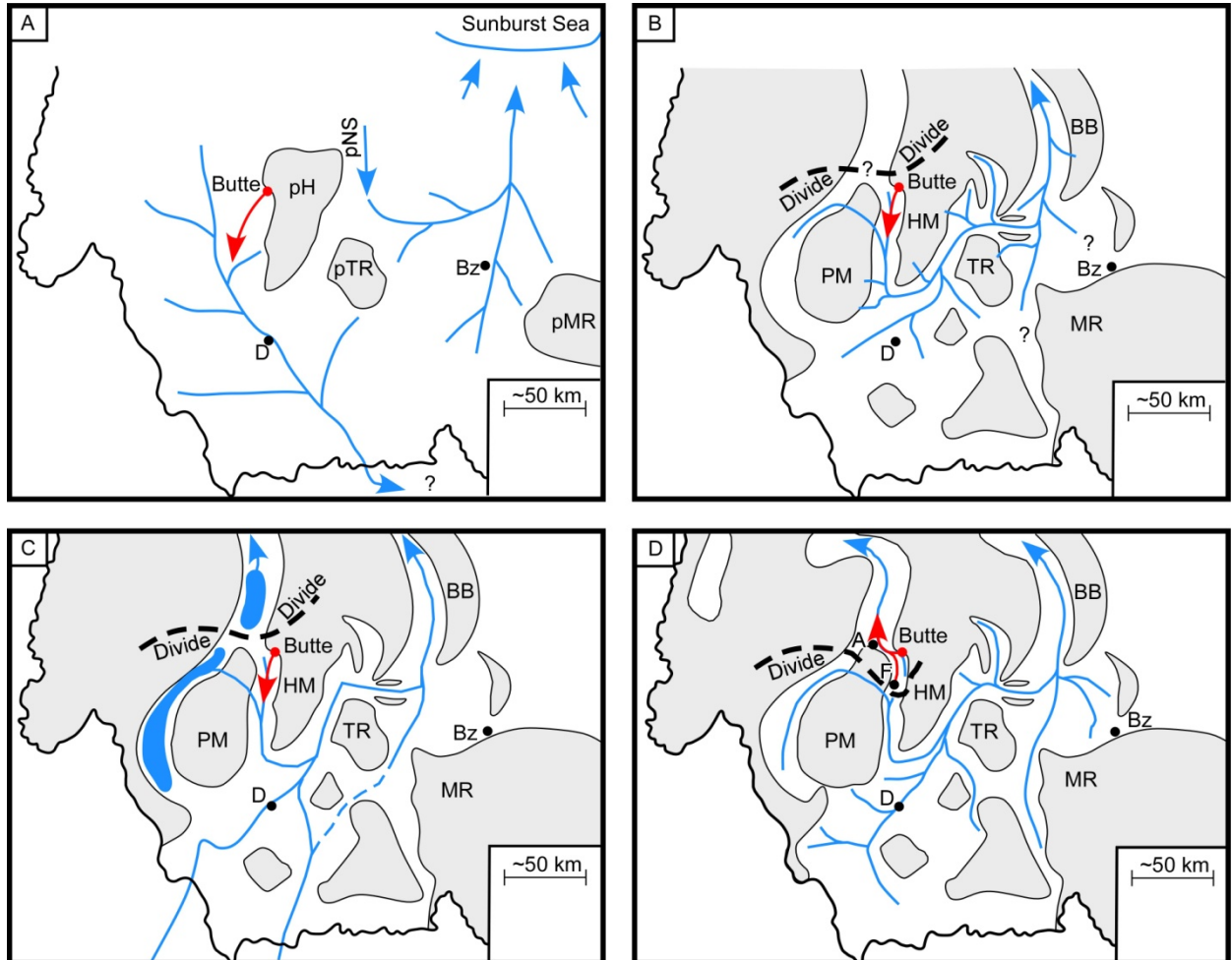


**Figure 4.** Paleogeographic evolution of southwestern Montana.

Figure 4 shows distribution of auriferous gravel derived from Butte in four time series (modified from DeCelles, 1986; Janecke, 1994; Sears et al., 2009; Schwartz and Schwartz, 2013): A. Early Cretaceous to Late Paleocene, B. Late Paleocene to middle Miocene, C. Middle Miocene to late Neogene, D. late Neogene to Present. Abbreviations: A = Anaconda; Bz = Bozeman; D = Dillon; F = Feeley; pH = proto-Highland Mountains; pMR = proto-Madison Range; pNB = proto-North Boulder Basin; pTR = proto-Tobacco Root Mountains; BB = Big Belt Mountains; HM = Highland Mountains; MR = Madison Range; PM = Pioneer Mountains; TR = Tobacco Root Mountains.

**Period 4 – Late Neogene to Present:** Perhaps as a consequence to deformation along the McCartney fault zone, the drainage divide shifted south to an area near Feeley, adding Silver Bow Creek to the north flowing Clark Fork drainage system (Fig. 4D; Ruppel, 1993; Ruppel et al., 1993; Vuke, 2004; Schwartz and Schwartz, 2013). As a result, Silver Bow Creek transported auriferous gravels westward through the Rocker basin to Anaconda, then northward through the Deer Lodge graben by way of the Clark Fork River. Downcutting and reworking of the older sediments in the area north of the divide to Silver Bow Creek concentrated detrital gold within the active channels and tributaries of Sand Creek and Canada Creek. At Butte, minor (~0.038 km) unroofing of the lode vein ore body transported ~21 tons of gold into the active fluvial system (Fig. 2B, 4D).

Conventionally, placer-source mass balance calculations conservatively estimate that 10 to 50% of gold eroded from a source is retained in the associated placer fields. However, the amount of placer gold recovered at Butte represents 0.7% of the total amount of gold eroded from the source, suggesting that ~17.9 Mtoz (558 t) gold was removed from the system. The model outlined above predicts that the majority of the gold (~75%) was eroded from the deposit and conveyed southward into the late Paleocene to early Eocene ancestral Beaverhead drainage system. Sediments capped by the early Eocene Lowland Creek volcanics are age equivalent to this period of greatest placer development. Source erosion slowed with the initiation of extensional faulting, renewed volcanism, and basin development during the Eocene. The initiation of middle Miocene Basin and Range-type normal faulting likely preserved but deeply buried auriferous gravels of Eocene to middle Miocene age within deep basins, beyond the reach of economic recovery. During the middle Miocene minor placer deposits developed proximal to the source. Fluvial reworking of the older sediments slightly concentrated detrital gold within active channels and were the target of the placer miners. These findings not only develop a predictive temporal and spatial distribution model of auriferous gravels derived from the district, more importantly, they help to explain why the expectations of the early prospectors were not fully realized.

## References

- Czehura, S., 2006, Butte: A world class ore deposit: *Mining Engineering*, v. 58, p. 14–19.
- DeCelles, P., 1986, Sedimentation in a tectonically partitioned, nonmarine foreland basin: The Lower Cretaceous Kootenai Formation, southwestern Montana: *Geological Society of America Bulletin*, v. 97, p. 911–931.
- Dilles, J., Einaudi, M., Proffett, J., and Barton, M.D., 2000, Overview of the Yerington porphyry copper district: Magmatic to nonmagmatic sources of hydrothermal fluids, their flow paths, alteration effects on rocks, and Cu-Mo-Fe-Au ores: *Society of Economic Geologists Guidebook Series*, v. 32, p. 55–66.
- Gottfried, Rowe, and Tilling, 1972, Distribution of Gold in Igneous Rocks, U.S. Geological Survey, Professional Paper 727, 42p.

- Gruen, G., Heinrich, C.H., and Schroeder, K., 2010, The Bingham Canyon porphyry Cu-Mo-Au deposit. II. Vein geometry and ore shell formation by pressure-driven rock extension: *Economic Geology*, v. 105, p. 69–90.
- Gustafson, L., and Hunt, J., 1975, The porphyry copper deposit at El Salvador, Chile: *Economic Geology*, v. 70, p. 857–912.
- Houston, R.A., and Dilles, J.H., 2013a, Structural Geologic Evolution of the Butte District, Montana: *Economic Geology*, v. 108, no. 6, p. 1397–1424.
- Houston, R.A., and Dilles, J.H., 2013b, Geology of the Butte mining district, Montana: Montana Bureau of Mines and Geology Open-File Report 627, 1 sheet, 1:24,000 scale.
- Janecke, S.U., 1994, Sedimentation and paleogeography of an Eocene to Oligocene rift zone, Idaho and Montana: *Geological Society of America Bulletin*, v. 106, p. 1083–1095.
- Long, K., 1995, Production and reserves of Cordilleran (Alaska to Chile) porphyry copper deposits, *in* Pierce, F., and Bolm, J., eds., *Porphyry copper deposits of the American Cordillera*: *Arizona Geological Society Digest*, v. 20, p. 35–68.
- McLaughlin, W.C., 1934, Auriferous Tertiary Gravels Near Rucker, in Silver Bow County, Montana: Unpublished B.Sc. thesis, Butte, Montana, Montana College of Mineral Science and Technology, 31p.
- Proffett, J.M., 2003, Geology of the Bajo de la Alumbrera porphyry copper-gold deposit, Argentina. *Economic Geology*, v. 98, p. 1535–1574.
- Reed, M., Rusk, B., and Palandri, J., 2013, The Butte Magmatic-Hydrothermal System: One Fluid Yields All Alteration and Veins: *Economic Geology*, v. 108, p. 1379–1396.
- Ruppel, E.T., 1993, Cenozoic tectonic evolution of southwest Montana and east-central Idaho: *Montana Bureau of Mines and Geology Memoir* 65, 62 p.
- Ruppel, E.T., O'Neill, J.M., and Lopez, D.A., 1993, Geologic map of the Dillon 1°x2° quadrangle, Idaho and Montana: U.S. Geological Survey Miscellaneous Investigations Series Map I-1803-H, 1:250,000 scale.
- Ruppel, E.T., O'Neill, J.M., and Lopez, D.A., 1993, Geologic map of the Dillon 1°x2° quadrangle, Idaho and Montana: U.S. Geological Survey Miscellaneous Investigations Series Map I-1803-H, 1:250,000 scale.
- Rusk, B., Reed, M., and Dilles, J., 2008, Fluid inclusion evidence for magmatic-hydrothermal fluid evolution in the porphyry copper- molybdenum deposit at Butte, Montana: *Economic Geology*, v. 103, p. 307–334.
- Schwartz, T., and Schwartz, R., 2013, Paleogene postcompressional- intermontane basin evolution along the frontal Cordilleran fold-and-thrust belt of southwestern Montana: *Geological Society of America Bulletin*, v. 125, no. 5-6, p. 961-984.

- Sears, J.W., and Fritz, W.J., 1998, Cenozoic tilt domains in southwestern Montana: Interference among three generations of extensional fault systems: Geological Society of America Special Paper 323, p. 241–247.
- Sears, J.W., and Ryan, P.C., 2003, Cenozoic evolution of the Montana Cordillera: Evidence from paleovalleys, *in* Flores, R.M., and Reynolds, R., eds., Cenozoic Systems of the Rocky Mountain Region: Rocky Mountain Section SEPM (Society for Sedimentary Geology), Denver, Colorado, p. 135–155.
- Sears, J., Hendrix, M., Thomas, R., and Fritz, W., 2009, Stratigraphic record of the Yellowstone hotspot track, Neogene Sixmile Creek Formation grabens, southwest Montana: Journal of Volcanology and Geothermal Research, v. 188, p. 250–259.
- Sillitoe, R.H., 2010, Porphyry copper systems: Economic Geology, v. 105, p. 3–41
- Thomas, R.C., 1995, Tectonic significance of Paleogene sandstone deposits in southwestern Montana: Northwest Geology, v. 24, p. 237-244.
- Vuke, S., 2004, Geologic map of the Divide Area, SW Montana, MBMG Open-File Report 502.
- Weed, W., 1912, Geology and ore deposits of the Butte district, Montana: U.S. Geological Survey, Professional Paper 74, p. 3–57.

# Boron Minerals of Western Montana—Occurrences and Ore Deposit Models

*Bruce E. Cox, Geologist / Consultant, Missoula, Montana*

In western Montana, authigenic boron minerals, especially tourmaline, occur principally in Cretaceous igneous rocks and Proterozoic sedimentary rocks. Tourmaline is a common gangue mineral in ore deposits of the Boulder batholith and overlying Elkhorn Mountains volcanics; ludwigite, ferroaxinite and dumortierite are less common. The spatial pattern of boron mineral occurrences and associated ore mineral assemblages suggest a genetic link between the Cretaceous ore deposits and the structural environment of the Proterozoic Belt basin.

## Introduction

The abundance of tourmaline in igneous rocks of the Boulder batholith terrain was first recorded in the early 1900s and has since been the subject of much interest. Adolf Knopf (1913) gives considerable detail on the quartz-tourmaline-sulfide mineral gangue and quartz-tourmaline wallrock alteration of northern Boulder batholith veins. Several recent studies have described tourmalinites in Proterozoic Belt rocks and their association with stratiform massive sulfide deposits (Beatty et al., 1987; Slack, 1993; Turner et al., 1992).

Objectives of this study are: (1) to review the more detailed historic descriptions of boron mineral occurrence, (2) to catalogue Montana boron mineral occurrences by deposit type and structural control and (3) to investigate a potential genetic link among deposits. Data are gleaned from numerous government and professional society publications and the author's field investigations files. The "Minerals of Montana" compilation of Larry French (2005) was the most comprehensive resource for locating boron mineral occurrences.

For convenience, the following abbreviations are used throughout this paper:

TGM = tourmaline group minerals, Kev = Elkhorn Mountains volcanics, Bqm = Butte quartz monzonite, NBT = northern Boulder batholith tourmaline trend.

## Boron Mineralogy

*Tourmaline*. -  $X Y_3 Z_6 B_3 Si_6 O_{27} (O, OH, F)_4$  - Tourmaline is, by far, the most abundant and most widely distributed boron mineral in western Montana. It is common within the Boulder batholith and Elkhorn Mountains volcanics (Figure 1) and less common in Archean and Proterozoic rocks.

**Figure 1.** *Tourmaline rosettes in pyritized aplite dike from flanks of the Pen Yan vein, Jefferson County, Montana.*



With few exceptions, Montana's geologic literature typically refers to the macroscopically black, crystalline or massive variety as tourmaline or shorl and does not distinguish between tourmaline group species. Dravite and elbaite are the only other TGMs reported to occur in Montana (French, 2005).

Dumortierite. -  $\text{Al}_7(\text{BO}_3)(\text{SiO}_4)_3\text{O}_3$  - The occurrence of dumortierite in Montana is rare but has been noted in pegmatites, Archean metamorphic rocks, and as part of a metasomatic mineral assemblage at Bqm / Kev contacts (Figure 2).



**Figure 2.** Dumortierite (blue) from Jack Creek Ridge, Jefferson County, Montana. The polished slab is approx. 3 cm wide.



Ludwigite. -  $\text{Mg}_2\text{Fe}^{3+}\text{BO}_5$  - Ludwigite is rare but is noted in magnetite bodies within marbles of the contact metamorphic aureoles of the Philipsburg batholith (Figure 3) and Boulder batholith (Emmons & Calkins, 1913 and Knopf, 1942, respectively).

**Figure 3.** Ludwigite from Philipsburg Mining District, Granite County, Montana. Specimen is approximately 2.5 cm in each dimension.

Ferroaxinite. -  $\text{Ca}_2\text{Fe}^{2+}\text{Al}_2\text{B}\text{Si}_4\text{O}_{15}(\text{OH})$  - Pegmatites and skarns are the host rocks for Montana's few ferroaxinite occurrences.

Habit. The macroscopic character of TGMs ranges from coarse prismatic crystals in breccia pipes and pegmatites to acicular or needle-like crystals in veins and aplites (Figure 4). Large tourmaline crystals have been observed in the open spaces or boxwork of veins. Crystal rosettes and thin, felt-like films are common. Tourmaline habit locally grades from fine to coarse at the contacts between aplite and pegmatite (Knopf, 1913).



(a)



(b)



(c)



(d)

**Figure 4.** Examples of tourmaline mineral habit, western Montana: (a) clast-supported breccia with quartz-tourmaline matrix, Skyline Mine, Jefferson County, (b) pegmatite with tourmaline, albite and quartz, Pipestone Pass, Jefferson County, (c) tourmaline-pyrite +/- quartz veins, Blizzard Mine, Jefferson County, (d) tourmaline-pyrite-quartz vein, Lucky Joe Mine, Lewis and Clark County; tourmaline xls approx. 3 mm long.

Knopf (1913) notes that in the Rimini district, tourmaline occurs in the veins with quartz and ore minerals and "...along one wall or the other by what is termed locally a ledge of black quartz ... an intergrowth of [fine-grained] quartz and black tourmaline. Locally this rock resembles a black jasperoid." It is likely that tourmaline "jasperoid" is common throughout the Bqm and Kev but has not been identified owing to its microscopic habit.

There has been very little description or research on the chemical composition of Montana TGMs, probably due to the apparent lack of gem-quality species or known industrial uses.

### **Modes of boron mineral occurrence—regional context**

Global occurrence of boron minerals in metallic ore deposits is nearly exclusive to tin-bearing griesens, breccias in veins and pipes and in volcanic or sedimentary stratiform deposits (Dietrich, 1985). In western Montana, authigenic boron mineral occurrences are concentrated in the northern half of Kev / Bqm terrain and in lower Proterozoic Belt basin rocks. Minor tourmaline occurrences have been noted in the Archean pegmatites near Bozeman (Heinrich, 1948) and in quartzites in southern Ravalli County (Berg, 1977). Emphasis is not given to the latter occurrences since they are not intimately associated with metallic mineralization.

*Veins.* Shear zone veins in the northern Boulder batholith and satellite intrusions (Figure 5) have recorded significant production of silver, gold, and base metals. Vein gangue is commonly comprised of quartz-tourmaline-pyrite +/- calcite-siderite; sulfide minerals are galena, sphalerite, chalcopyrite and arsenopyrite. In most districts, silver is the dominant commodity. Gold accounts for a greater proportion of vein production in the Rimini and Elliston districts where vein tourmaline and wallrock tourmalization are most common.

The rarity of this concentration of tourmaline-bearing polymetallic veins is highlighted by Knopf's observation (1913) that metal production from the Alta mine alone (Wickes district) was probably greater than any other known tourmaline-bearing vein deposit worldwide.



Breccia Pipes. Steeply dipping elliptical breccia pipes are clustered near the southeast and northwest end of the Bqm / Kev tourmaline-bearing vein trend (Figure 5). Each pipe is a clast-supported breccia with quartz-tourmaline +/- sulfide matrix; a pyritic wallrock alteration halo is noted at two pipes. Tourmaline is the only recorded boron mineral and occurs as black prismatic crystals in radiating splays and free-standing crystals in vugs (Figure 6). Albite may constitute a significant portion of breccia matrices in the Elliston district pipes.

Gold is the dominant commodity and occurs as coarse isolated grains (Figure 6) and probably as microscopic inclusions in pyrite. Gold and silver values were approximately equal at the Elkhorn Queen mine, the only producer of the tourmaline breccia pipe group.



**Figure 6.** Kev breccia from Elliston Mining District, Powell County. Image shows breccia matrix of tourmaline-quartz-sericite (after albite?); native gold grain near center photo.

Intrusive Contacts. Boron metasomatism driven by igneous intrusion is indicated by tourmaline and/or dumortierite concentrations at the roof of Bqm, the margins of large sill-like aplite bodies, and in dioritic dikes.

Aplites and Pegmatites. Tourmaline is common in pegmatites throughout the Boulder batholith and in pegmatites of Archean age (Heinrich, 1948) as free-standing crystals and as acicular or needle-like coatings or inclusions in quartz (Figure 7). Ferroaxinite and elbaite have been reported in a few locations in the Boulder batholith.



**Figure 7.** Tourmaline needles in amethystine quartz, Pohndorf pegmatite, Jefferson County.

Stratiform Deposits. Proterozoic tourmalinite and tourmaline breccia form the footwall rocks of the Sullivan mine massive sulfide deposit at Kimberly, British Columbia. Deliberate exploration for and in bedded Proterozoic tourmalinites was performed in western Montana by several mining companies in the 1980s. Tourmalinite occurrences are most common in middle Proterozoic rocks along the axis of Belt Basin exposures (Figure 8).

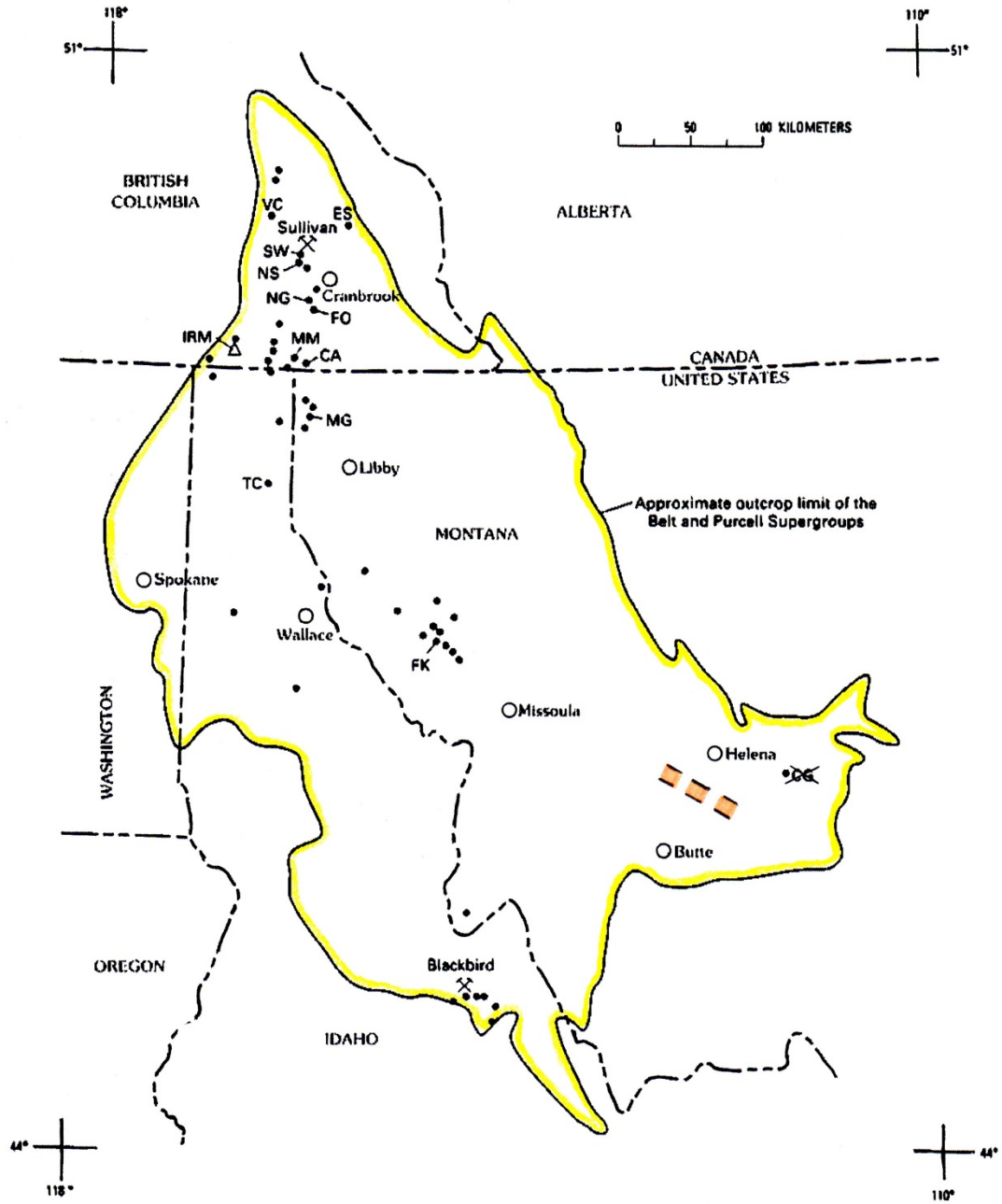


**Figure 8.** Tourmalinites in Proterozoic Rocks of Montana, Idaho, and British Columbia. Modified from Slack, 1989. The Northern Boulder Batholith Tourmaline Trend is shown in orange.

## Precursor boron mineralization—A proposed model

This paper proposes a structural history in which: (1) the NBT is a northwest-trending wrench fault system reactivated during late Cretaceous but seated in Precambrian basement and (2) this fault system provided a sub-basin and feeder for seafloor brine-pool mineral deposition in middle Proterozoic time (Figure 9).

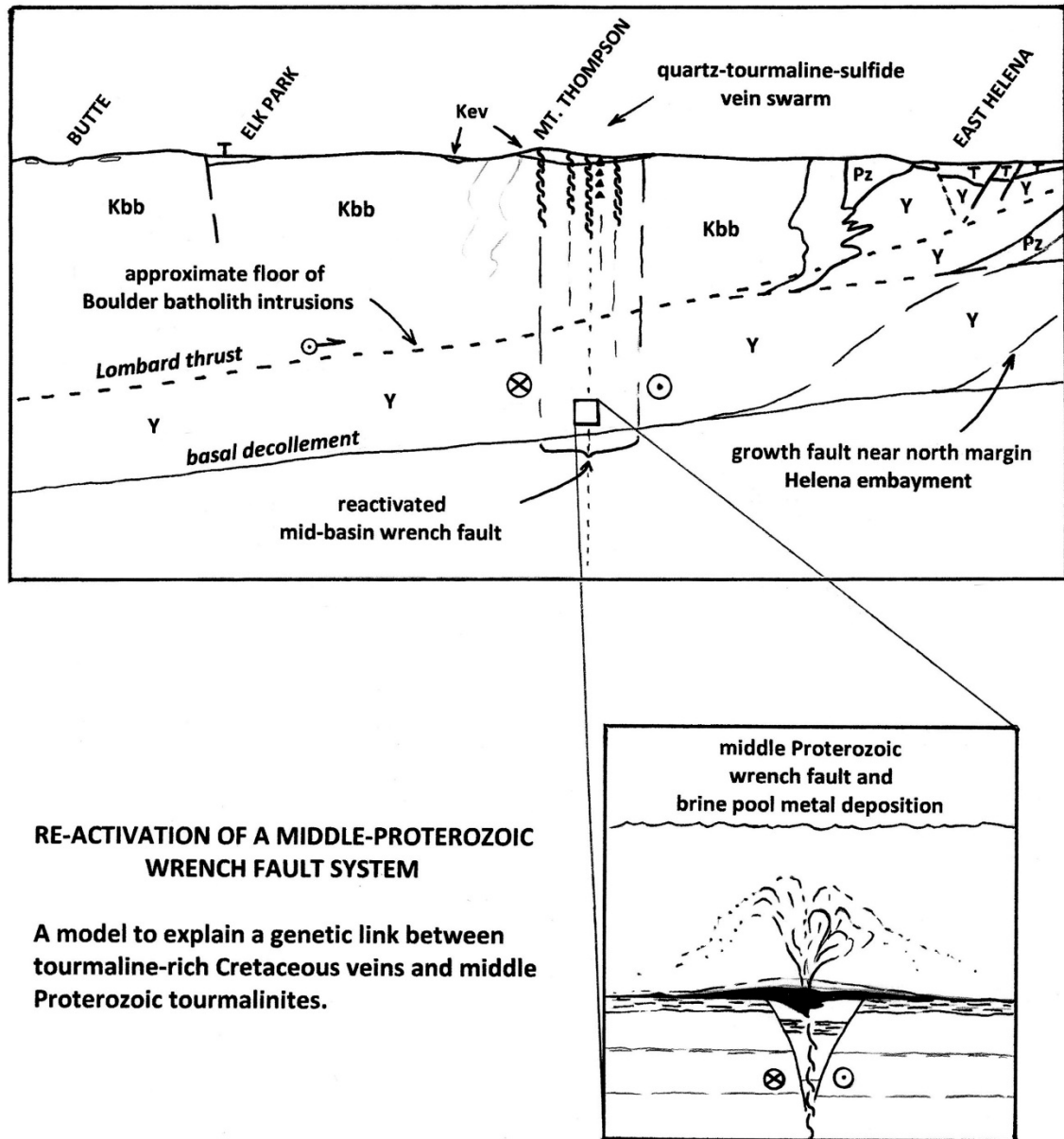
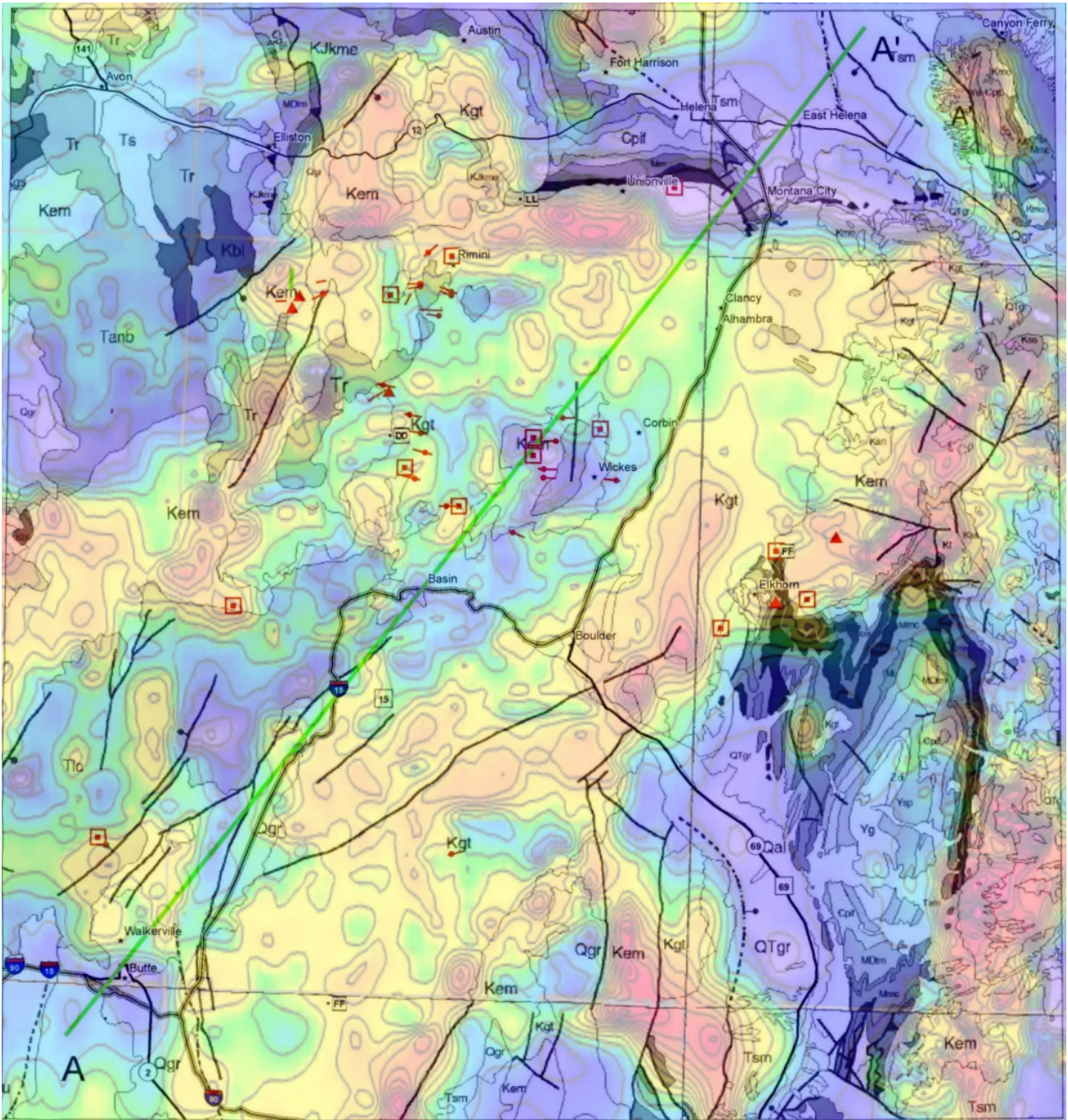


**Figure 9.** Re-activation of a middle-Proterozoic wrench fault system. A model to explain a potential genetic link between tourmaline-rich Cretaceous veins and middle-Proterozoic tourmalinites. The line of section for A–A' is shown on Figure 5. Thickness of Boulder Batholith intrusions and depth to principal structures is modeled from Burton et al., 1999, Plate 3; no vertical exaggeration.

Structural Framework. Wrench faulting reactivated through younger crystalline rocks would yield a prominent shear fabric. Most tourmaline-bearing veins in the northern Boulder Batholith are contained within steep-dipping-to-vertical shear zones, some with continuous strike exposure greater than 6 kilometers and locally greater than 40 meters wide. The NBT trend may have structural continuity northwestward along the Lewis and Clark Line expressed by numerous thrusts and normal faults along the northeast crest of the Garnet Range.

The NBT is centered between the north and south margins of the Proterozoic Helena embayment and conforms to a center-basin northwest trend of tourmalinite occurrences in Prichard equivalent rocks (Figure 8). Tourmaline is not recorded in metal deposits beyond the southeast end of the NBT or in the eastern limit of the Belt basin.

The NBT trend shows axial symmetry with an aeromagnetic trough and local steep magnetic gradients in the otherwise broad magnetic high of the Boulder batholith and Elkhorn Mountains volcanics terrain (Figure 10). This trough is interpreted to be the signature of surficial and concealed alteration of igneous rocks along the NBT and northwest–southeast extensions of the suspect reactivated wrench fault.



Index Map and Explanation shown on Figure 5

**Figure 10.** Aeromagnetic map of the northern Boulder Batholith terrain superimposed on Figure 5 of this report. Data modeled by W.I. Van der Poel. The data of McCafferty et al., 1998 were reprocessed and imaged to enhance middle amplitude and wavelength of response.

*Ore Deposit Production and Associated Mineralogy.* Production figures, mineralogy and trace elements of the NBT veins and Sullivan mine deposit are shown in Table 1. The two districts have comparable alteration and ore mineralogy and associated principal trace elements.

**Table 1. Production and Geochemical Data for the Sullivan Mine and NBT Mining Districts**

	<b>Sullivan<sup>1</sup></b>	<b>NBT<sup>2</sup></b>
Ore Tons (million)	134	2.4
Silver Production (oz/ton)	2	6.6
Lead Production (%)	6.5	1.7
Zinc Production (%)	5.6	0.8
Ore minerals	galena, sphalerite, pyrrhotite, pyrite	galena, sphalerite, pyrite, arsenopyrite
Alteration minerals	tourmaline, albite, chlorite pyrite	tourmaline, pyrite, arsenopyrite
Trace metals	Sn, As, Sb, Bi	As, Bi, Sn

1 - Summary data from Turner, 1992.

2 - Compiled for Elkhorn, Colorado, Basin, Rimini, and Elliston districts from Roby, 1960; McClernan, 1983; McClernan, 1976.

The much higher ratio of silver to base metals in the NBT deposits may be due to greater chemical mobility of silver in the Cretaceous hydrothermal environment.

Minerals rich in tin and bismuth are well documented in the Sullivan mine region and are common in the northern Boulder batholith. Cassiterite as botryoidal “wood tin” was locally abundant in the placer deposits mined near the headwaters of Basin Creek and Tenmile Creek (the center of the NBT trend) and in the Prickly Pear Creek gold dredge operations (Ruppel, 1963). However, no greisens or other tin-bearing protoliths have been discovered in the region. Tin may have weathered directly from the upper (eroded) levels of the shear veins.

Bismuth (+/- tellurium) may provide a similar Cretaceous / Proterozoic link. The few known western Montana occurrences of bismuthinite and native bismuth are almost all in northern Boulder batholith rocks.

*Age Dating.* Proterozoic dates from NBT ores would bolster the hypothesis that the Cretaceous veins are linked to Proterozoic mineralization. U/Pb zircon analyses (TIMS and SHRIMP) have become the preferred methods for evaluating the age of intrusions and mineralization in the Boulder Batholith (Lund et al., 2002). Zircons extracted from Boulder batholith intrusive rocks are typically xenocrystic, showing overgrowths on distinct cores which commonly yield Precambrian inheritance in the range of 1700 Ma to 2700 Ma. Similarly, zircons from Main Stage veins in the Butte district (no tourmaline gangue) yield Precambrian inheritance and Cretaceous mineralization dates. <sup>40</sup>Ar/<sup>39</sup>Ar zircon dating on sericite from three NBT vein samples gave 73–81 Ma mineralization dates but no zircon xenocrysts have been dated. The tourmalinized aplites and tourmaline jasperoids flanking NBT veins may yield suitable material for U / Pb or Pb / Pb dating.

## Summary and implications

An unusual concentration of boron minerals, especially tourmaline, occurs in shear zone vein deposits, breccia pipes, and metasomatic rocks of the Cretaceous northern Boulder batholith terrain. These metal deposits may have formed within a reactivated wrench fault system that initially fed stratiform silver-base metal mineralization in a Proterozoic basin. The proposed genetic link is supported by the trends of: Cretaceous tourmaline-bearing veins and Proterozoic tourmalinites, aeromagnetic data, trace element geochemistry, and by limited U-Pb zircon dating. Further confirmation of the NBT model may prove helpful in identifying reactivated basement structures and mineralized source protoliths beneath or adjacent to thick cover. The world-class veins and porphyry system of the Butte district, although geochemically boron-poor, may have developed within a similar reactivated Proterozoic wrench fault system.

## Acknowledgments

Many thanks to Tony Van der Poel and Ted Antonioli for review and discussion of the manuscript and to Larry Johnson for preparation of maps and figures. Several dead ends were averted with the help of Karen Lund and Jerry Zieg.

## References

- Beatty, D.W., Hahn, G.A., and Threlkeld, W.E., 1988, Field, isotopic and chemical studies of tourmaline-bearing rocks in Belt-Purcell Supergroup: genetic constraints and exploration significance for Sullivan type ore deposits: *Canadian Journal of Earth Science*, Vol. 25, p. 392–408.
- Becraft, G.E., Pinckney, D.M., and Rosenblum, S., 1963, *Geology and Mineral Deposits of the Jefferson City Quadrangle, Jefferson and Lewis and Clark Counties, Montana*: U.S. Geological Survey Professional Paper 428, 100 p.
- Burton, B.R., Lageson, D.R., Schmidt, C.J., Ballard, D.W., and Warne, J.R., 1999, Large-magnitude shortening of the Lombard thrust system Helena Salient Montana fold and thrust belt: implications for the emplacement of the Boulder batholith and reconstruction of the Belt basin, *in* R. Berg, ed., *Proceedings of Belt Symposium III*, Montana Bureau of Mines and Geology Special Publication 112, p. 25–35, Plate 3.
- Dietrich, R.V., 1985, *The Tourmaline Group*: Van Nostrand Reinhold Company, 300 p.
- du Bray, E.A., Aleinikoff, J.N., and Lund, K., 2012, *Synthesis of Petrographic, Geochemical and Isotopic Data for the Boulder Batholith, Southwest Montana*: U.S. Geological Survey Professional Paper 1793, 39 p.
- French, L.B., 2005–2009, *Minerals of Montana, Parts I–V*: Montana Bureau of Mines and Geology Open-File Report 519.

- Heinrich, E.W., 1948, Pegmatite Mineral Deposits of Montana: Montana Bureau of Mines and Geology Memoir 28, 56 p.
- Klepper, M.R., Weeks, R.A., and Ruppel, E.T., 1957, Geology of the Southern Elkhorn Mountains, Jefferson and Broadwater Counties, Montana: U.S. Geological Survey Professional Paper 292, 82 p.
- Knopf, A., 1913, Ore Deposits of the Helena Mining Region: U.S. Geological Survey Bulletin 527, 143 p.
- Knopf, A., 1942, Ludwigite from Colorado Gulch near Helena, Montana: American Mineralogist, vol. 27, p. 824–825.
- Lund, K., et al., 2002, SHRIMP U-Pb and  $^{40}\text{Ar}/^{39}\text{Ar}$  Age Constraints for Relating Plutonism and Mineralization in the Boulder Batholith Region, Montana: Economic Geology, Vol 97, p. 241–267.
- McCafferty, A., Bankey, U., and Brenner, K.C., 1998, Montana Aeromagnetic and Gravity Maps and Data: U.S. Geological Survey Open-File Report 98-333.
- McClerman, H.G., 1976, Metallic Mineral Deposits of Powell County, Montana: Montana Bureau of Mines and Geology Bulletin 98, 69 p.
- McClerman, H.G., 1983, Metallic Mineral Deposits of Lewis and Clark County, Montana: Montana Bureau of Mines and Geology Memoir 52, 73 p.
- Roby, R.N., Ackerman, W.C., Fulkerson, F.B., and Crowley, F.A., 1960, Mines and Mineral Deposits (Except Fuels) Jefferson County, Montana: Montana Bureau of Mines and Geology Bulletin 16, 122 p.
- Ruppel, E.T., 1963, Geology of the Basin Quadrangle, Jefferson, Lewis and Clark and Powell Counties, Montana: U.S. Geological Survey Bulletin 1151, 121 p.
- Slack, J.S., 1993, Models for tourmalinite formation in the Middle Proterozoic Belt and Purcell supergroups (Rocky Mountains) and their exploration significance: Geological Society of Canada Current Research, Part E, Paper 93-1E, p. 33–40.
- Turner, R.J.W., Hoy, T., Leitch, C.H.B., and Anderson, D., 1992, Guide to the tectonic, stratigraphic and magmatic setting of the Middle Proterozoic stratiform sediment-hosted Sullivan Zn-Pb deposit, southwestern British Columbia: British Columbia Ministry of Energy, Mines and Petroleum Resources Information Circular 1992-23, 53 p.
- Vuke, S.M., Porter, K.W., Lonn, J.D., and Lopez, D.A., 2007, Geologic Map of Montana, Edition 1.0: Montana Bureau of Mines and Geology Geologic Map 62.

## **Elevated REE in Ore Minerals of the Pryor Mountain Mining District, South Central Montana**

*Anita Moore-Nall and David R. Lageson; Montana State University, Department of Earth  
Science, Bozeman, Montana*

Rare Earth elements (REE) lanthanums to lutetium (atomic numbers 57–71) are members of Group IIIB on the periodic table, and all have similar chemical and physical properties. The elements Sc and Y (atomic numbers 21 and 39) are also Group IIIB elements for which the REE substitutes are often included in REE lists. REE are actually fairly common in the continental crust but are rarely concentrated in mineable deposits (Sutherland et al., 2013), with the LREE being more commonly concentrated than the HREE.

REE are significantly concentrated within the uraninite from breccia pipes in northern Arizona (Wenrich et al., 2013) in both LREE and especially in the HREE. The Pryor Mountain mining district of south central Montana and the Little Mountain Mining district of northern Wyoming host uranium vanadium deposits similar to the Colorado Plateau uranium breccia pipe deposits in Arizona (Van Gossen et al., 1996). The Montana and Wyoming deposits are orders of magnitude smaller in scale and the primary ore minerals are what are usually considered secondary uranium ore minerals occurring in the oxidized zones of U-V deposits: tyuyamunite  $\text{Ca}(\text{UO}_2)_2(\text{VO}_4)_2 \cdot 5-8\text{H}_2\text{O}$  and metatyuyamunite  $\text{Ca}(\text{UO}_2)_2(\text{VO}_4)_2 \cdot 3-5\text{H}_2\text{O}$ . Minor amounts of a few other uranium minerals identified in the Pryor Mountain mining district include: autunite  $\text{Ca}(\text{UO}_2)_2(\text{PO}_4)_2 \cdot 10-12\text{H}_2\text{O}$  (Warchola and Stockton, 1982), uranophane  $\text{Ca}(\text{UO}_2)_2\text{Si}_2\text{O}_7 \cdot 6\text{H}_2\text{O}$  and apple green liebigite  $\text{Ca}_2(\text{UO}_2)(\text{CO}_3)_3 \cdot 11\text{H}_2\text{O}$  from the East Pryor mine (Patterson et al., 1988), francevillite  $(\text{Ba,Pb})(\text{UO}_2)_2(\text{VO}_4)_2 \cdot 5\text{H}_2\text{O}$  (Moore-Nall and Lageson, 2013), davidite  $(\text{Fe}^{+2}, \text{La}, \text{U}, \text{Ca})_6 (\text{Ti}, \text{Fe}^{+3})_{15} (\text{O}, \text{OH})_{36}$  from the Dandy mine (Warchola and Stockton, 1982), and possibly samarskite-Yb  $(\text{Yb}, \text{Y}, \text{Fe}^{3+}, \text{Fe}^{2+}, \text{U}, \text{Th}, \text{Ca})_2 (\text{Nb}, \text{Ta})_2 \text{O}_8$  from the East Pryor mine and bastnasite  $(\text{Ce}, \text{La})(\text{CO}_3)\text{F}$  from the Old Glory mine (Moore-Nall, unpublished data). Gangue minerals include hematite, limonite, iron-hydroxides, radioactive green calcite, dolomite, golden and white barite, gypsum, white and dark purple fluorite, pyrite, marcasite, opal, quartz, including herkimer style quartz (Moore-Nall and Lageson, 2011), and clay minerals.

Rare Earth elements were detected by SEM at Montana State University in some of the minerals from the Pryor Mountain mining district. Additionally analyses performed by American Analytical Services Inc., in Osborn, Idaho by ICP-MS of yellow uranium vanadium ore minerals from the Sandra mine in the Pryor Mountain mining district reveal a cumulative REE content of 2097 ppm (raw data, not converted to oxide values). All the REE (Sc and Y were not analyzed) were detected in the prepared pulp from the Sandra mine. The cumulative LREE portion of this analysis is 1489 ppm, with cerium (Ce) representing 1280 ppm and samarium (Sm) 74.5 ppm. The HREE cumulative portion of the analysis is 608 ppm, with all the elements being greater than 15 times average crustal abundance except Dysprosium (Dy), which was only about 5 times greater. Gangue minerals fluorite and barite were also analyzed from other mines in the district.

Dark purple fluorites from the East Pryor mine and the Dandy Mine were analyzed as well as a golden barite from the Swamp Frog Mine. The fluorites contained La, Ce, Pr, Nd, Sm, Eu, Gd, Dy, Ho, Er, and Yb in concentrations ranging from 1.03 to 9.54 ppm, while barite had only 11.1 ppm Eu. Splits from the Sandra mine UV sample, a UV prospect site, the Dandy mine fluorite sample, and a barite sample from the Old Glory mine sample were analyzed for Au by American Analytical Services, Inc. by Fire Assay ICP Finish. The samples contained 0.031, 0.055, 0.067, and 2.35 ppm (detection limit 0.005 ppm) respectively.

The Pryor Mountain Mining District, Montana and the Little Mountain Mining District, Wyoming were prospected and mined for uranium and vanadium from 1956 to the late 1970s. The deposits are hosted in mineralized collapse breccia features in the top 190–240 ft paleokarst horizon of the Mississippian aged Madison Limestone. Both districts are located in Laramide structures. Relatively small, high-grade (median grades of 0.36%  $U_3O_8$ , 0.41%  $V_2O_5$ ) deposits in Montana and Wyoming, combined, produced 223,000 pounds of uranium oxide ( $U_3O_8$ ) from 19 properties and 236,000 pounds of vanadium oxide ( $V_2O_5$ ) from 15 properties during the peak production years (Patterson et al., 1988). In addition to being stratigraphically localized, the uranium deposits in the area of Red Pryor Mountain show a structural relationship to a zone of fractures that trend N. 65° W, on a trend that includes the East Pryor and Little Mountain group of mines (Patterson et al., 1988); mineralization appears to be enhanced where NW-striking fractures intersect the crest of the south-plunging Gypsum Creek anticline (Blackstone, 1974). Furthermore, the alignment of mines (Old Glory, Sandra, Lisbon, Perc Group, Dandy, Marie, and Swamp Frog) on the Red Pryor quadrangle is spatially coincident with a reverse fault in the basement that subtends the south-plunging Gypsum Creek anticline (Blackstone, 1974).

Two main schools of thought exist relative to the origin of uranium in these ore deposits. McEldowney et al., 1977, proposed that the uranium deposits in the Madison Limestone were formed by meteoric waters. Uranium-bearing meteoric water, principally groundwater, is proposed to have leached uranium from Tertiary tuffaceous rocks that once covered the region prior to epeirogenic uplift and exhumation, and then deposited uranium in preexisting karst solution cavities through deep circulation in the upper Madison Limestone. The second school of thought proposes that these deposits formed by structurally controlled, ascending hydrothermal fluids (Warchola and Stockton, 1982). Their interpretation was that hydrothermal fluids ascended along major fault or fracture zones along the eastern edge of Big Pryor Mountain and anticlinal structures of the Little Mountain District. The characteristics of both mining districts strongly suggest a bottom-up hydrothermal origin, including breccia pipes or chimneys and breccia networks that follow bedding surfaces and vertical fractures, hydrothermal mineral assemblage associations, vug-filling character of mineralization, and alteration of country rocks, including bleaching and Liesegang banding. Sources of vanadium are also uncertain, with two possible sources (Patterson et al., 1988) which might also be the sources for the REE. Vanadium may have originated in the Park City Formation (Love, 1961; 2003), or from vanadium-rich oil (Stone, 1967) that may have seeped up from depth from the Bighorn Basin along fractures into these structures.

## References

- Blackstone, D.L., Jr., 1974, Preliminary geologic map of the Red Pryor Mountain 7.5' quadrangle, Carbon County, Montana: Montana Bureau of Mines and Geology Open-File Report 68, 1:24,000.
- Love, J.D., 1961, Vanadium and associated elements in the Phosphoria Formation in the Afton area, western Wyoming: U.S. Geological Survey Professional Paper 424C, p. C279–C282.
- Love, J.D., 2003, Vanadium deposits in the Lower Permian Phosphoria Formation, Afton area, Lincoln County, western Wyoming: U.S. Geological Survey Professional Paper 1637, 28 p.
- McEldowney, R.C., Abshier, J.F., and Lootens, D.J., 1977, Geology of uranium deposits in the Madison Limestone, Little Mountain area, Big Horn County, Wyoming, *in* Veal, H.K., ed., *Exploration frontiers of the Central and Southern Rockies: Rocky Mountain Association of Geologists*, p. 321–336.
- Moore-Nall, A.L., and Lageson, D.R., 2011, Herkimer diamonds in the Pennsylvanian Tensleep Formation may indicate hydrothermal influences for mineralization of the Red Pryor Mountain uranium/vanadium deposits: Geological Society of America, Abstracts with Programs, Vol. 43, No. 5, p. 599.
- Moore-Nall, A.L., and Lageson, D.R., 2013, Francevillite [(Ba,Pb)(UO<sub>2</sub>)<sub>2</sub>(V<sub>2</sub>O<sub>8</sub>)•5H<sub>2</sub>O] identified in the Uranium Vanadium deposits in the Pryor Mountain Mining District, Montana and the Little Mountain Mining District, Wyoming may provide a link to the elevated lead in the Bighorn River and be related to fluid migration of the Lower Kane Cave, Wyoming: Geological Society of America, Abstracts with Programs, Vol. 45, No. 7, p. 198.
- Patterson, C.G., Toth, M.I., and Kulik, D.M., 1988, Mineral resources of the Pryor Mountain, Burnt Timber Canyon, and Big Horn Tack-On Wilderness Study Areas, Carbon County, Montana and Big Horn County, Wyoming: U.S. Geological Survey Bulletin 1723, 15 p.
- Sutherland, W.M., Gregory, R.W., Carnes, J.D., and Worman, B.N., 2013, Rare Earth Elements in Wyoming: Wyoming State Geological Survey (WSGS) Report of Investigation No. 65. ISBN: 978-1-884589-59-1
- Van Gosen, B.S., Wilson, A.B., and Hammarstrom J.M., 1996, Mineral Resource Assessment of the Custer National Forest in the Pryor Mountains, Carbon County, South-Central Montana: U.S. Geologic Survey Open-File Report 96-256, 69 p.
- Warchola, R.J., and Stockton, T.J., 1982, National Uranium Resource Evaluation, Billings quadrangle, Montana: U.S. Department of Energy publication No. PGJ/F-015(82), 33 p.
- Wenrich, K.J., 2013, Rare Earth Elements in Arizona, *in* P. Richardson and R. Grant, eds., *Minerals of Arizona 21<sup>st</sup> Annual Symposium*, 12 p.

## Silver Mineralogy of the Butte Mines

*Chris Gammons and Ryan Stevenson, Department of Geological Engineering, Montana Tech, Butte, MT 59701,*

Based on published records (U.S. Bureau of Mines, Montana Resources), the Butte mining district produced nearly 700 million ounces of silver between 1882 and 2004. This ranks Butte second in total U.S. silver production, behind the Coeur d'Alene district, Idaho. Based on the USGS global database for total production + reserves, Butte ranks 3<sup>rd</sup> in the world for silver endowment amongst porphyry Cu deposits, after Chuquicamata and Escondida. Although much has been written about the famous copper-rich Main Stage veins of Butte, as well as the pre-Main Stage porphyry Cu-Mo mineralization, there is little published information on the mineralogy of the silver-rich veins of Butte. The senior author of this presentation (CG) has been compiling what is known on Butte silver production and mineralogy, while at the same time preparing new polished sections (with help from RS and other graduate students) of Ag-rich ore specimens from the archived Anaconda Mining Company (AMC) Collection on the Montana Tech campus. The new sections are being analyzed by optical microscopy, SEM, and micro-Raman spectroscopy. The aim of this unfunded project is to slowly assemble a comprehensive set of polished sections that documents the ore mineralogy of Butte.

Silver mineralization in Butte falls into three broad categories: 1) as Ag(I)-Cu(I) solid solutions within Cu-sulfide minerals (especially chalcocite, covellite, bornite, enargite, tennantite); 2) as Ag-rich minerals formed during supergene enrichment of the Main Stage veins; and 3) as primary Ag-bearing sulfide and sulfosalt minerals in the Main Stage veins. Primary Ag-bearing minerals include pearceite, pyrargyrite, argentite (Ag<sub>2</sub>S), stromeyerite (CuAgS), Ag-bearing tetrahedrite, and very rare electrum (to date only found in one sample from the Marget Ann mine, near the extreme north end of the district). In the supergene enrichment zone, acanthite and/or stromeyerite can replace pre-existing sulfide minerals (e.g., galena), or, if no sulfides are present, silver may precipitate as the native metal.

Despite the fact that most discrete, primary silver minerals are found in mines of the outer portions of the district, much of the Ag production in Butte came from the Cu-rich Main Stage veins and Berkeley Pit, where discrete Ag minerals are very rare. Based on the study of Brimhall et al. (Econ. Geol., 1984), Cu-sulfide minerals of Butte locally contain well over 1000 ppm of silver. The overall Ag:Cu ratio for Butte is estimated to be roughly 1:1000, indicating that each wt% of copper contains roughly 100 ppm (or close to 3 oz/ton) of Ag. On an annual basis, the Ag:Cu ratio of Butte ore has decreased over the 120 years of mining history, reflecting trends in mining methods combined with the metal zonation within the district.

## **Revised Model for Carbonate-Hosted Proterozoic Hydrothermal Talc Deposits in Southwest Montana**

*S.J. Underwood, Senior Geologist, Childs Geosciences, Bozeman, Montana*

Southwest Montana talc ( $\text{Mg}_3\text{Si}_4\text{O}_{10}(\text{OH})_2$ ) deposits in Pre-Belt marbles are associated with Proterozoic hydrothermal systems. The older published model taps sea water for talc formation in shallow-to-near surface environments, where hydrothermal plumbing systems along faults were fueled by crystallizing dikes and sills intruded into a Belt Basin sediment veneer. Botryoidal talc textures, vugs, and mineral replacements are cited as evidence of shallow formation. New findings (since the mid-1990s) have been perfunctorily added into this model rather than carefully evaluated to see whether some of the basic ideas in the old model should be revisited (e.g., Underwood et al., 2014). In particular, the pressure and temperature conditions outlined in the old model might produce some talc in a very few cases, but are unlikely to yield the volumetrically significant deposits presently mined in the Ruby Range by Barretts Minerals Inc. and in the Gravelly Range by Imerys Talc.

This work marks an effort to recast the model for site-specific hydrothermal systems to a more generalized set of regional conditions that might generate large talc ore bodies. Starting from a geochemical data perspective, hot hydrous fluids are assumed to react with the buried marbles in the Ruby, Greenhorn, and Gravelly Ranges. Gammons and Matt (2002) analyzed fluid inclusions in quartz pods within talc from two deposits near the Yellowstone Mine, and applied geothermometry to the brine to establish a 190–250 °C temperature range, and geobarometry to the chemical composition of extracted fluids to estimate the 3.5–10.5 km entrapment depth range. They concluded that connate brines may have penetrated faults and reacted with the marbles and metasediments to produce talc and chlorite. In the Ruby Range, a brine temperature of ~250°C is permitted by applying a new lower temperature talc-brine stable isotope geothermometer (Saccocia et al., 2009) to talc  $\delta^{18}\text{O}$  and  $\delta\text{D}$  values from mine samples (Brady et al., 1998). The equilibrium fluid calculated for talc appears to better fit connate basin brines rather than sea water.

Presently, no Belt sediments are found across this portion of the Dillon Block, and indeed this region is seldom postulated to have had any Belt sediments overlying the crystalline pre-Belt basement. However, if subsidence of the Lemhi subbasin extended across this region, an accumulation of sediments temporally equivalent to the Missoula Group (ca. 1450 to 1250 Ma) may have been deposited. In the area of Glacier Park, Montana, the Missoula Group of the Mesoproterozoic Belt basin achieved thicknesses up to 5.5 km. Using oxygen isotope geothermometry for equilibrium quartz and illite grains, Eslinger and Savin (1973) calculated temperatures between 225 and 310 °C for burial diagenesis and normal geothermal gradient for the Missoula Group. If these conditions were applicable to SW MT, the thickest sediment deposition on the lower elevation portions of the Dillon Block may have been in an embayment

extending from the Regal, Treasure/Beaverhead Mines to the Yellowstone Mine. A single  $^{40}\text{Ar}/^{39}\text{Ar}$  date for sericite next to talc yielded  $\sim 1.36$  Ga (Brady et al., 1998) might reflect time required for sediment accumulation, and development of hydraulic conditions to circulate hot connate basin brines.

A hypothetical structure for the regional connate brine aquifer might be: (1) complexly folded and sheared zones of marble sandwiched within schist and gneiss layers on Paleoproterozoic metasediments over Archean basement rocks beneath (2) saprolitized metasediments and regolith shed during unroofing the Big Sky Orogen (i.e., Tobacco Root Mountain area) through which (3) diabase dikes (from crustal extension) fed a basaltic volcanic field. This surface was variably eroded and formed a base for Missoula Group equivalent Belt sediments. The geothermal basin brines had sufficient time to develop unique chemical and stable isotopic signatures as deep connate fluids. In the low permeability carbonate zones, hot hydrothermal fluids became channelized by fractures or discontinuities.

To create large deposits of microcrystalline talc, hydraulic fracturing in the marbles would provide a mechanical means to promote extensive talc formation despite the slow reaction kinetics at relatively low temperature. (The slow diffusion-controlled processes likely responsible for some mineral replacements by talc could still occur.) Hydraulic fracturing at great depths is possible where reservoirs have high fluid overpressure that approaches lithostatic pressure such that marble tensile strength is routinely reached (Secor, 1965). Hydrofracturing of the marble and horizons within it and at the contacts with various gneisses and schists might be generated in several ways, but a crack-seal mechanism might have been the highest yielding talc forming process. Each break in the marble would likely rupture at the weakest points and the invading hot brine would carry reactive fluid to the fresh surfaces and remove fluid-mobile products. This water dominated system would enable the transport of minor constituents to the fresh surface for reaction, and preserve delicate structures in the protoliths because only small volumes would react at any given time. Next to the continuous talc bodies, talc pods, blebs, and/or stringers could form at reactive sites that had (or developed) access to fluids as tectonic activity and dissolution progressed. Chlorite could form where Al activity was elevated. Dynamic hydraulic fracturing could have been sustained for long times or periodically restarted. Finally, because weathering and erosion have removed the hypothetical lithologic sequence over this area, acceptance, modification, or rejection of this model will require additional geoscientific investigations.

## Acknowledgments

C. Walby, M. Cerino, D. Berg, J. Childs. CGI provided financial support.

## References

- Anderson, D.L., Mogk, D.W., and Childs, J.F., 1990, Petrogenesis and timing of talc formation in the Ruby Range, southwestern Montana: *Economic Geology and the Bulletin of the Society of Economic Geologists*, v. 85, p. 585–600, doi:10.2113/gsecongeo.85.3.585.
- Brady, J.B., Cheney, J.T., Rhodes, A.L., Vasquez, A., Green, C., Duvall, M., Kogut, A., Kaufman, L., and Kovaric, D., 1998, Isotope geochemistry of Proterozoic talc occurrences in Archean marbles of the Ruby Mountains, Southwest Montana, U.S.A.: *Geological Materials Research, Mineralogical Society of America*, v. 1, no. 2, p. 1–41.
- Eslinger, E.V., and Savin, S.M., 1973, Oxygen isotope geothermometry of the burial metamorphic rocks of the Precambrian Belt Supergroup, Glacier National Park, Montana: *Geological Society of America Bulletin*, v. 84, p. 2549–2560.
- Gammons, C.H., and Matt, D.O., 2002, Using fluid inclusions to help unravel the origin of hydrothermal talc deposits in southwest Montana: *Northwest Geology*, v. 31, p. 41–53.
- Saccocia, P.J., Seewald, J.S., and Shanks, W.C., III, 2009, Oxygen and hydrogen isotope fractionation in serpentine–water and talc–water systems from 250 to 450 °C, 50 MPa: *Geochimica et Cosmochimica Acta*, v. 73, p. 6789–6804.
- Secor, D.T., Jr., 1965, Role of fluid pressure in jointing: *American Journal of Science*, v. 263, p. 633–646.
- Underwood, S.J., Childs, J.F., Walby, C.P., Lynn, H.B., Wall, Z.S., Cerino, M.T., and Bartlett, E., 2014, The Yellowstone and Regal talc mines and their geologic setting in southwestern Montana, *in* Shaw, C.A., and Tikoff, B., eds., *Exploring the Northern Rocky Mountains: Geological Society of America Field Guide 37*, p. 161–187, doi:10.1130/2014.0037(08).

## **Boulder Batholith Pegmatites**

*William C. (Chris) van Laer, ASTERISM Services, Butte, Montana*

The Boulder batholith is a granitic intrusive composed of several plutons in southwest Montana. Its age has been given as late Cretaceous to early Tertiary, and it is surrounded by older sediments and meta-sediments of various ages and also late Tertiary lake bed deposits. The composition of the Boulder Batholith varies from true granite to more basic granodiorite, but is generally quartz monzonite.

Fine-grained bodies and segregations of aplite are common in certain areas, and are generally associated with roof facies and appear to be magmatic segregations of lighter elements and materials that rose to the roof of the plutons. These are generally flat-lying bodies, discontinuous, but sometimes tabular with well-defined boundaries. In some of these units, local segregations of coarse-grained pegmatites indicate a slower cooling rate than that of the aplites themselves, which are considered to be the result of rapid cooling of the granites.

Boulder Batholith pegmatites have compositions roughly similar to the host rock; that is, some are quartz monzonite pegmatites, but the great majority of these are rich in silica and quartz, as true granite pegmatites. Basic mineralogical composition in descending order of abundance would normally be quartz, microcline or orthoclase, albite, and schorl tourmaline, with lesser amounts of magnetite, pyrite, muscovite, ilmenite, and other species.

Locally many of these pegmatitic bodies are rich in volatile elements, that is, elements and compounds that do not solidify upon crystallization of the magma. These volatiles include (but are not restricted to) hydrogen, oxygen, carbon dioxide, sulfur, phosphorus, and especially water. The result is that openings or voids form in the pegmatites in specific zones or areas of lower pressure, where the minerals grow into the voids uninterrupted by adjacent minerals (as euhedral crystals). Such crystals often have considerable value, as demonstrated by pegmatite deposits worldwide that produce crystals and gems of many types like aquamarine, elbaite tourmaline, topaz, and many others.

The pegmatites of the Boulder Batholith are generally considered to be syngenetic, that is, they formed during the consolidation and solidification of the granite itself, but a few seem to indicate cross-cutting relationships that would make them epigenetic bodies. An observation made on many of these aplite-pegmatite bodies is that there are little or no alteration zones along contacts or margins, indicating formation close to the time the magma began to cool.

The real interest in these pegmatites is in those euhedral minerals and crystals that are found in the vug openings or cavities (also called "pockets" by collectors). Among these species are smoky quartz crystals (some up to a meter or more in length), amethyst quartz, microcline, albite (including the variety cleavelandite, and a fine blue variety known only to this area), black tourmaline (schorl), epidote (in acicular sprays or divergent clusters of needle-like crystals), titanite (or sphene, sometimes in euhedral crystals of huge proportions up to ten inches across), axinite, danburite, apatite, topaz, beryl, phenakite, and other species. One feature of the local mineralogy that is prominent is the occurrence of various inclusions in quartz crystals: perhaps

more varieties of this occur here than any other single locality in the world. Inclusions that have been identified in quartz crystals (euhedral quartz) so far include: tourmaline, epidote, goethite, allanite, hematite, anthophyllite, pyrite, anatase, cosalite, rutile, and beryl var. aquamarine. Other highlights of local minerals are very large apatite crystals ("fragments" of which measured over 5 inches across); amethyst as scepters and clusters of tiny crystals with numerous inclusions of goethite ("onegite"); world-class phenakites, some doubly-terminated and attached to schorl tourmaline crystals; beautiful gemmy, golden-colored topaz crystals; small but colorful elbaite tourmalines (in green, pink, purple, and deep red hues); huge titanite crystals, always twinned and colored from honey-yellow to lime green; exceptional amethyst "scepters" with stems of smoky or tourmalinated quartz and heads of deep purple amethyst; and some of the finest quality and color amethysts, comparable to any other locality in the world.

The pegmatites of the Boulder Batholith have been exploited in such deposits as the famous Pohndorf Amethyst mine and the nearby Little Gem mine, both for amethyst and amethyst scepters; also the lesser-known Gem Queen mine northwest of Whitehall, Montana along the eastern margin of the batholith, where spectacular titanite crystals were once found, along with fine schorl tourmaline, allanite, and scheelite crystals. Other smaller deposits have produced numerous examples of local treasures and many have yet to be discovered.

## **Reserve Definition and Geology, Continental Pit, Butte Montana**

*Steve Czehura, Montana Resources, LLP, Butte, MT*

The Continental pit is situated immediately east and north of the city of Butte in the foothills of the Continental Divide. Ongoing mining utilizes drill-blast and shovel-truck unit operations typical for bulk tonnage extraction to sustain an ore feed of 49,000 tpd. After two stages of crushing and two stages of grinding, copper and molybdenum concentrate products are recovered by froth flotation in the Butte Concentrator and sold to traders, who sell these concentrates to smelters and roasters. Butte is centrally located relative to the world markets with transportation to continental North American smelters and roasters as well as seacoast facilities around the world. About 62% of Montana Resources' revenue comes from sulfide copper sales, 4% from by-product silver, 3% from copper precipitation, and 31% from molybdenum.

Over the past five years an aggressive "Deposit Definition Drilling Program" incorporating diamond coring and RVC drilling totaling some 229,000 feet has more than doubled known mining reserves. This exploratory drilling east of the Continental Fault defined minable copper-molybdenum reserves down to the 4,480 elevation.

The current R24 Pit Design detailed utilizing MineSight's Pit Optimizer, indicates proven and probable reserves of 756 MM tons with a favorable strip ratio, averaging 0.24% copper and 0.031% molybdenum with a 0.074 opt silver credit. With this design, allowing the Continental pit to go deeper, some 31 MM tons averaging 0.60% copper were relegated to the resource category to avoid the Pittsmont Number 2 Shaft leaving a 300 foot pillar (offset) at the 5,480 elevation in the highwall of the final pushback. Mining will eventually progress downward to 4,600 elevation exploiting deep enrichment immediately west of the Continental Fault.

In the Continental area, Butte Quartz Monzonite is host to low-grade, porphyry style, copper and molybdenum mineralization exposed at surface in the footwall of the Continental Fault. This style of mineralization was intercepted by underground workings beneath the Berkeley pit at about the 2,000 level. Subparallel strands of the Continental Fault, collectively thought to have as much as 3,500 feet of dip-slip displacement, are exposed, along strike, in the bottom reaches of the Continental pit and in "cross section" in the north highwall. The deposit is bounded on the west by the Continental Fault and on the East by the Klepper Fault. In the Butte District, two mineralizing events are recognized as important relative to reserve definition: Pre-Main Stage (PMS) and Main Stage (MS). The Pre-Main Stage veinlet swarms and crackles with distinctive secondary green biotitic selvages, typify the potassium feldspar metasomatism associated with the early quartz-chalcopyrite-molybdenite porphyry style mineralization. Swarms of barren quartz, molybdenite crackles (slicks), and various styles of banded quartz-molybdenite veinlets marked the end of the Pre-Main Stage event and set the structural pattern for the classic mesothermal Main Stage veining to follow. These east to northeasterly trending, steeply dipping, massive copper sulfide veins, characterized by wide sericitic envelopes, often offset by conjugate northwest trending MS veins with gouge in both the hanging wall and footwall, sustained the historic underground mining in Butte, but occur only as small veinlets in

the Continental pit. The bulk of the Continental orebody that sustains ongoing mining was mineralized by interlacing Pre-Main Stage crackles and veinlet swarms. Deepening of the current pit continues to exploit this mineralization. Ongoing research over the past 30 years, however, has further quantified another facet of Butte geology that is important to reserve definition. As a result of deep drilling in the District, a massive quartz-sericite-pyrite plug was delineated at depth in the southeast corner of the Berkeley pit that was contemporaneous with MS mineralization. It is thought that fluids from this intrusive mixed with meteoric water and sericitized a massive area above the PMS porphyry system. The swarms of pyrite and quartz-pyrite veinlets associated with this intervening mineralization prepared the ground for subsequent supergene copper enrichment that occurred with ongoing weathering as the district was uplifted and faulted by the mountain building processes along the Rocky Mountain Front. These events produced the copper enrichment blankets conformable with ancient ground water tables both east and west of the current Continental pit. The upper eastern pushback visible from uptown Butte is scheduled to expose near-surface enriched reserves between the current Continental pit and I-15 over the next 5 years. The enrichment blanket between the Continental pit and the Berkeley pit is scheduled for exploitation mid-2050, allowing mining to progress downward to the ultimate design depth mid-2060.

## **Some constraints on the origin of Montana sapphire deposits**

*Richard B. Berg, Montana Bureau of Mines and Geology*

Sapphires were first discovered in Montana in alluvial deposits along the Missouri River near Helena in 1865. Subsequent sapphire discoveries, all by gold miners, followed near Rock Creek in the area west of Philipsburg and along the South Fork of Dry Cottonwood Creek east of Deer Lodge. Sapphires were also discovered in the Yogo deposit, an ouachitite dike, near Lewistown that is the only significant bedrock sapphire deposit in Montana. From about 1900 until the late 1930s large quantities of sapphires were produced for the watch bearing market. Since the production of synthetic sapphire and loss of this market sapphires have been mined for the gemstone market. Historic production of sapphires in Montana exceeds 70 tonnes with more than 90 percent of this production from the Rock Creek district.

The following is a summary of our knowledge of Montana sapphire deposits that has been compiled from many sources in the hope that it will assist in our explaining the large concentration of sapphires in Montana.

### **Bedrock sources of sapphires**

**Lithology**—The indicated sources for alluvial sapphires in the Rock Creek district and the South Fork Dry Cottonwood Creek are volcanic rocks of rhyolitic to dacitic composition. A sill that contains sapphires in low concentrations situated along the Missouri River near Helena is a trachybasalt, and the Yogo dike is an ouachitite. The bedrock source for the Missouri River sapphire deposits in the Helena area is not yet known.

**Age**—All of the known and indicated bedrock sources are Eocene igneous rocks. Specifically the volcanics in the Rock Creek district are 50 Ma old (Berg, 2014). The Lowland Creek Volcanics, the probable source for the sapphires in the South Fork of Dry Cottonwood Creek, range in age from 48.6 to 52.9 Ma (Dudas and others, 2010). The sill along the Missouri River is 50.8 Ma old (Irving and Hearn, 2003) and the Yogo dike is 48.6 Ma (Harlan, 1996).

### **Evidence for magmatic transfer**

Sapphires from all three major alluvial deposits (Rock Creek, South Fork of Dry Cottonwood Creek, and the Missouri River) show evidence of resorption. Resorption features are particularly pronounced on the surfaces of sapphires from the South Fork of Dry Cottonwood Creek where deep grooves are developed along the basal and rhombohedral parting planes (Berg, 2007). Sapphires from the three major alluvial deposits differ significantly in surface morphology attributed to resorption (Berg and Equall, 2013). Features caused by abrasion are typically minimal.

### **Evidence for a metamorphic source rock**

Giuliani and others (2005) have shown that  $\delta^{18}\text{O}$  values can be used to differentiate between magmatic and metamorphic sapphires. Sapphires from the Rock Creek district and the South Fork of Dry Cottonwood Creek have  $\delta^{18}\text{O}$  values less than 7 ‰, within the range of metamorphic sapphires (Berg and others, 2008).

### **Evidence for a crustal origin**

Evidence for a crustal origin for these alluvial sapphires is based on mineral inclusions. Mineral inclusions are compatible with amphibolite-facies metamorphism (see Berg, 2007, 2014; Garland, 2002; and Williams and Waters, 2004 for lists of mineral inclusions). Cade and others (2006) concluded on the basis of geochemistry of included garnets that the Yogo sapphires are from a mantle eclogite.

### **Conclusions and speculation**

Comparison of the distribution of Montana sapphire occurrences and crustal terranes (Sims and others, 2004) shows that most of these occurrences are underlain by the Paleoproterozoic Wallace terrane. The Wallace terrane is interpreted by Sims and others to be an ocean-arc terrane separated from the Archean terrane to the southeast by a zone referred to as the Trans Montana Orogen. It is speculated that most corundum of the gem variety was derived from the Wallace metamorphic terrane and carried to the surface by Eocene volcanism.

### **References**

- Berg, R.B., 2007, Sapphires in the Butte-Deer Lodge area, Montana: Montana Bureau of Mines and Geology Bulletin 134, 59 p.
- Berg, R.B., 2014, Sapphires in the southwestern part of the Rock Creek sapphire district, Granite County, Montana: Montana Bureau of Mines and Geology Bulletin 135, 86 p.
- Berg, R.B., and Equall, N., 2013, Comparison of surface morphology of Montana alluvial sapphires by SEM [abs.]: Geological Society of America Abstracts with Programs, v. 45, no. 7, p. 525–526.
- Berg, R.B., Gammons, C.H., and Arehart, G.B., 2008, Preliminary oxygen isotope values for Montana sapphires [abs.]: Geological Society of America Abstracts with Programs, v. 40, no. 6, p. 254.
- Cade, Andrea, and Groat, L.A., 2006, Garnet inclusions in Yogo sapphires [abs.]; 2006 Gemological Research Conference, Gems and Gemology, v. XLII, p. 106.
- Dudas, F.O., Ispolatov, V.O., Harlan, S.S., and Snee, L.W., 2010,  $^{40}\text{Ar}/^{39}\text{Ar}$  geochronology and geochemical reconnaissance of the Eocene Lowland Creek Volcanic field, west-central Montana: The Journal of Geology, v. 118, no. 3, p. 295–304.

- Garland, M.I., 2002, The alluvial sapphire deposits of western Montana: Ontario, University of Toronto, Ph.D. dissertation, 381 p., 4 maps.
- Harlan, S.H., 1996, Timing of emplacement of the sapphire-bearing Yogo dike, Little Belt Mountains, Montana: *Economic Geology*, v. 91, p. 1159–1162.
- Irving, A.J., and Hearn, B.C., Jr., 2003, Alkalic rocks of Montana: kimberlites, lamproites, and related magmatic rocks, *in* Guidebook prepared for the VIIIth International Kimberlite Conference, Montana Field Trip, 16–21 June 2003, Kjarsgaard, B.A., ed., Ottawa, Geological Survey of Canada.
- Sims, P. K., O'Neill, J.M., Bankey, V., and Anderson, E., 2004, Precambrian basement map of Montana—An interpretation of aeromagnetic anomalies: U.S. Geological Survey Scientific Investigations Map 2829.
- Williams, T.J., and Walters, L., 2004, Mineral inclusions in alluvial sapphires from Browns Gulch, southwestern Montana; Implications for the origin of Montana alluvial sapphires [abs.]: *Geological Society of America Abstracts with Programs*, v. 36, no. 5, p. 225.